JGR Space Physics

RESEARCH ARTICLE
10.1029/2024JA033086

Special Collection:
Recent Discoveries in Substorm Research

Investigating the Spatiotemporal Development of Substorm Expansion Phase Aurora: Successive Onsets or Poleward Boundary Intensifications?

Sneha Yadav[1], Larry R. Lyons[1], Yukitoshi Nishimura[2], Jiang Liu[1,3], Sheng Tian[1], Ying Zou[4], and Eric F. Donovan[5]

[1]Department of Atmospheric and Oceanic Sciences, University of California, Los Angeles, Los Angeles, CA, USA, [2]Department of Electrical and Computer Engineering and Center for Space Physics, Boston University, Boston, MA, USA, [3]Department of Earth, Planetary, and Space Sciences, University of California, Los Angeles, Los Angeles, CA, USA, [4]Johns Hopkins University Applied Physics Laboratory, Laurel, MD, USA, [5]Department of Physics and Astronomy, University of Calgary, Calgary, AB, Canada

Abstract Following the auroral substorm onset, the active aurora undergoes expansion, which can vary in spatial and temporal extent. The spatiotemporal development of the expansion phase active aurora is controlled by new auroral intensifications that often follow the initial onset. Using seven examples, we investigate the nature of these new auroral intensifications and address a question: are they new auroral onsets, that is, "successive onsets" or poleward-boundary intensifications (PBIs) and ensuing auroral streamers? We observed events that included both types of auroral features—successive onsets and PBIs—and their combinations. For multiple-onset substorms, successive onsets may occur eastward, westward, and poleward of the initial onset, resulting in a diverse range of expansion phase spatial extent and durations. Single-onset substorms show only one auroral onset, but their spatiotemporal development can resemble that of multiple-onset substorms. However, the additional activations are mainly PBIs and subsequent streamers. In some cases, PBIs undergo explosion, leading to a rapid poleward and azimuthal expansion of the aurora, resembling the auroral substorm onset. A prolonged sequence of PBIs and its longitudinal extension can contribute significantly to the spatiotemporal development of substorms expansion phase. Results suggest that post-onset flow channels drive the spatiotemporal development of the substorm expansion phase by (a) triggering successive onsets and (b) inducing bursts of PBIs and their prolonged sequence. We speculate that post-onset flow channels likely originate from the polar cap, but more evaluation is required. Our findings highlight the significance of examining imager data before solely relying on magnetometers to identify substorm onsets.

Key Points:

- Successive onsets, often preceded by post-onset streamers, cause diverse range of expansion phase coverage and durations
- A prolonged sequence of poleward-boundary intensifications and auroral streamers play a crucial role in driving spatiotemporal development of substorm expansion phase
- Post-onset flow channels play an important role in spatiotemporal development of substorm expansion phase

Supporting Information:

Supporting Information may be found in the online version of this article.

Correspondence to:

S. Yadav,
snehay@atmos.ucla.edu

Citation:

Yadav, S., Lyons, L. R., Nishimura, Y., Liu, J., Tian, S., Zou, Y., & Donovan, E. F. (2024). Investigating the spatiotemporal development of substorm expansion phase aurora: Successive onsets or poleward boundary intensifications? *Journal of Geophysical Research: Space Physics*, *129*, e2024JA033086. https://doi.org/10.1029/2024JA033086

Received 20 JUL 2024
Accepted 21 NOV 2024

Author Contributions:

Conceptualization: Sneha Yadav, Larry R. Lyons
Investigation: Sneha Yadav
Methodology: Sneha Yadav
Project administration: Larry R. Lyons
Resources: Eric F. Donovan
Software: Sneha Yadav, Jiang Liu, Sheng Tian
Supervision: Larry R. Lyons
Validation: Larry R. Lyons, Yukitoshi Nishimura
Visualization: Sneha Yadav, Larry R. Lyons
Writing – original draft: Sneha Yadav

1. Introduction

Auroral substorms, the visible part of magnetospheric substorms, are a phenomenon through which magnetospheric energy is deposited in the auroral ionosphere. Auroral substorm onset is identified by a sudden brightening of an auroral arc that lies near the equatorward boundary of the auroral oval in the midnight sector, followed by auroral breakup. Subsequently, the aurora intensifies and expands poleward, constituting the substorm expansion phase. The poleward expansion gives rise to a bulge of active aurora that often extends toward the west, forming the westward traveling surge (WTS) (Akasofu et al., 1965). Sometime after the disturbed auroral region reaches its maximum poleward position, auroral activity decreases, and the recovery phase begins. Different from auroral substorm, pseudo-breakups have a weak poleward expansion (<2° magnetic latitude, Aikio et al., 1999) that lasts only for a few minutes (<3 min, Nishimura, Lyons, Zou, Angelopoulos, & Mende, 2010).

The expansion phase activity is known to continue for a wide range of periods, ranging from several minutes to tens of minutes, and can extend over spatial areas varying from limited latitudinal and longitudinal extents to more than 10° of latitude and 100° longitude. This variety can be seen from numerous published examples (e.g., Despirak et al., 2011; Gjerloev et al., 2007; Ieda et al., 2016; Lyons, Nishimura, Donovan, & Angelopoulos, 2013; Lyons, Nishimura, Gallardo-Lacourt, et al., 2013; Nishimura et al., 2020; Perraut et al., 2003). Based on the ground magnetometer data, on average, the substorm expansion phase duration is typically 20–30 min (Chu et al., 2015; Forsyth et al., 2015; Gjerloev et al., 2007) and the recovery phase lasts 30–40 min on average (Chu et al., 2015; Forsyth et al., 2015). The larger the duration and spatial extent of a substorm expansion phase is, the larger should be the disturbances in the Earth's ionosphere-thermosphere system in terms of total energy

Writing – review & editing: Larry R. Lyons, Yukitoshi Nishimura, Jiang Liu, Sheng Tian, Ying Zou

deposition; therefore, it is important to understand the factors that control the spatiotemporal development of substorm expansion. Despite its importance, this topic has received only very limited attention in the past (Lyons & Nishimura, 2020 and reference therein).

During the expansion phase of a substorm, new auroral brightenings may occur, resulting in further discrete expansion of the substorm activity. This phenomenon is known as multiple-onset substorms (e.g., McPherron, 1979; Pytte et al., 1976; Rostoker et al., 1980). The auroral brightenings following the main onset have often been called "substorm intensifications" (Rostoker et al., 1980), though these intensifications may be new onsets, poleward boundary intensifications (PBIs, Lyons et al., 1999), or auroral streamers (e.g., Montbriand, 1971; Nakamura et al., 1993; Sergeev et al., 1999). Here, we refer to new auroral onsets following the main onset as the "successive onsets," and distinguish between such onsets, PBIs, and ensuing streamers. Another scenario is when more than one auroral substorm develops nearly simultaneously at different magnetic local times (MLT), forming double auroral bulges, which later merge into one large bulge (Ohtani et al., 2021). Multiple-onset substorms may lead to auroral expansions that progress poleward in a stepwise manner (Aikio et al., 2006; Ieda et al., 2016; Kisabeth & Rostoker, 1971, 1974; Sergeev & Yahnin, 1979; Wiens & Rostoker, 1975). Successive substorm onsets influence the intensity, duration, and spatial extent of the expansion phase aurora. On the other hand, auroral substorms that are not followed by any succeeding auroral onsets are referred to here as single-onset substorms.

PBI is a recurrent form of auroral intensification at the poleward boundary of the nightside auroral oval, a region often considered a proxy for the open-closed boundary. Auroral features that often extend equatorward from PBIs to lower latitudes are referred to as auroral streamers, which can be almost north-south aligned, and are considered as a crucial component of the expansion phase (Elphinstone et al., 1996; Henderson, 2012; Henderson et al., 1994, 1998; Montbriand, 1971; Nakamura et al., 1993, 2001; Nishimura, Lyons, Zou, Angelopoulos, & Mende, 2010; Sergeev et al., 1999, 2000, 2004; Yadav et al., 2022). They not only extend equatorward from the PBIs but also from the poleward boundary of the auroral bulge if the bulge has not yet reached the auroral poleward boundary. Abrupt and large ground magnetic field drops that occur during the expansion phase are often associated with PBIs and ensuing equatorward extending auroral streamers (Lyons, Nishimura, Donovan, & Angelopoulos, 2013; Yadav et al., 2022 and reference therein), and these extend westward with the westward propagating surge (Lyons, Nishimura, Gallardo-Lacourt, et al., 2013). The prolonged occurrence of PBIs and auroral streamers may influence the duration of the substorm expansion phase, a topic that has remained largely unexplored thus far.

One of the characteristic features of substorms is the occurrence of Pi2 pulsations (Olson, 1999; Saito et al., 1976), an ultralow-frequency phenomenon with periods ranging from 40 to 150 s (Jacobs et al., 1964). However, Pi2 pulsations observed from high to low latitudes appear to not be directly linked to substorm onset, but are associated with the onset of PBIs and auroral streamers, which often occurs soon after substorm onset (Kim et al., 2005; Lyons, Nishimura, Donovan, & Angelopoulos, 2013; Nishimura et al., 2012; Sutcliffe & Lyons, 2002; Yadav et al., 2022), indicating their connection to disturbances originating in the near-Earth magnetotail (Keiling & Takahashi, 2011). This highlights the importance of auroral observations in identifying substorm onset and auroral features such as PBIs and auroral streamers. In this study, we reinforce PBI and streamer observations with their associated Pi2 pulsations.

The highly variable spatial extent and duration of substorm expansion phase raises several unanswered questions: (a) What factors determine the spatial extent and duration of the substorm expansion phase? (b) Is multiple-onset the only plausible reason for the large spatial extent and duration of substorms? (c) Is a single-onset substorm longitudinally confined compared to multiple-onset substorms, or is it possible for a single-onset substorm to demonstrate a large spatial extent and duration of the expansion phase aurora? Addressing these questions is crucial for enhancing our understanding of substorms and the underlying phenomena that control their duration and spatial extent.

Although a stepwise evolution of the expansion phase aurora seems to be a common feature, to our knowledge, studies describing the characteristics of these substorm auroral intensifications and their role in driving the spatial extent (both azimuthal and poleward) and duration of substorms expansion phase are sparse. In this paper, we take advantage of the coverage of the North American auroral oval by the ground-based Time History of Events and Macroscale Interactions during Substorms (THEMIS) all-sky-imager (ASI) array (Donovan et al., 2006; Mende et al., 2008) of NASA's THEMIS program (Angelopoulos, 2008), which enables resolving the finer details of the auroral activity over a large area. We emphasize the role of successive onsets in spatiotemporal development of

the substorm expansion phase. We evaluate seven events, including, for comparison, examples of single onset substorms, with one having a broad and long duration substorm expansion phase without successive onsets but with a prolonged periods of expansion phase streamers and PBIs.

It is widely accepted that streamers are auroral manifestations of equatorward moving ionospheric flow channels (e.g., Gallardo-Lacourt et al., 2014), which correspond to earthward-moving flow bursts in the plasma sheet (Henderson et al., 1998; Kauristie et al., 2000; Nakamura et al., 2001; Sergeev et al., 1999; Zesta et al., 2000). Pre-onset streamers (Lyons et al., 2010; Nishimura, Lyons, Zou, Angelopoulos, & Mende, 2010; Nishimura, Lyons, Zou, Xing, et al., 2010) and their associated flow channels (Lyons, Gallardo-Lacourt, & Nishimura, 2022; Lyons, Liu, Nishimura, Reimer, et al., 2021; Lyons, Nishimura, et al., 2022) have been found to be a crucial element of the sequence of events that lead to substorm onset, indicating that the earthward penetration of flow bursts triggers substorms. It is known that earthward-propagating flow bursts are persistently injected from the magnetotail during substorms. Post-onset auroral streamers serve as a tool to track these expansion-phase flow bursts using ground-based measurements. The post-onset equatorward-extending auroral streamers have been shown to correlate with abrupt and significant decreases in the ground magnetic field (Yadav et al., 2022). However, the role of post-onset streamers in triggering successive substorm onsets has not yet been thoroughly explored.

2. Data Set and Methodology

We use THEMIS ASI images to identify auroral features. With 21 cameras, the THEMIS ASIs cover a large portion of the auroral oval in North America. Each imager has a latitudinal coverage of ∼9° and longitudinal coverage of ∼2.5 hr MLT. These imagers provide high spatial and temporal resolution (∼1 km spatial at the zenith and 3s temporal), allowing detection of weak, fast-evolving auroral forms and spatially extended auroral structures. To study the temporal variation of auroral features and their latitudinal motion, north-south (N-S) keograms are made using slices of auroral images along the central longitude of a station.

To examine the perturbations in the horizontal (H) component of magnetic field near the auroral activity, we used 1-min daily baseline subtracted ground magnetic field data from the SuperMAG (http://supermag.jhuapl.edu) database (Gjerloev, 2012). High-resolution magnetometer data (≤1 s) from the THEMIS ground-based magnetometer array are used to study the Pi2 pulsations at mid-latitudes in association with auroral activity. The Pi2 pulsations are derived by band-pass filtering of the H-component data with a passband of 40–150 s.

The solar wind parameters (interplanetary magnetic field (IMF) Bz, By) are obtained from the OMNI database. We used the SuperMAG auroral indices SML (analogous to AL, Gjerloev, 2012; Newell & Gjerloev, 2011) at a 1-min cadence. We used the Space Physics Environment Data Analysis Software (SPEDAS) tool (Angelopoulos et al., 2019) to download and analyze the geomagnetic indices and THEMIS ground-based magnetic field. Table S1 in Supporting Information S1 indicates the name, code, and geomagnetic coordinates of all the ground magnetometer stations used in this study.

3. Observations

We present seven examples with good auroral viewing selected to study the spatiotemporal development of single-onset and multiple-onset substorms. Substorm auroral onset is identified using auroral images, with the auroral onset marked by the initial brightening near the equatorward boundary of the auroral oval, often along a preexisting growth phase arc. Substorm auroral onsets occurring after the initial onset are referred to as successive onsets, and such events are termed "multiple-onset substorms." Apart from substorm onset, new auroral brightenings may occur, which could be associated with PBIs or auroral streamers. Rapid, latitudinally localized brightenings or the formation of new arcs along the poleward boundary of the auroral oval have been identified as PBIs. Auroral streamers are identified as approximately north-south aligned arcs that originate from the poleward boundary of the auroral oval or auroral bulge and extend equatorward. On some occasions, we observed auroral intensifications characterized by the rapid poleward and azimuthal expansion of the ongoing expansion phase aurora. These events have been referred to as auroral re-intensifications.

This section is subdivided into two parts: the first part describes the substorm onset consisting of just one onset, known as the single-onset substorm. The second part elaborates on the multiple-onset substorm resulting in the stepwise evolution of the expansion phase aurora. The first two single-onset substorms are not followed by

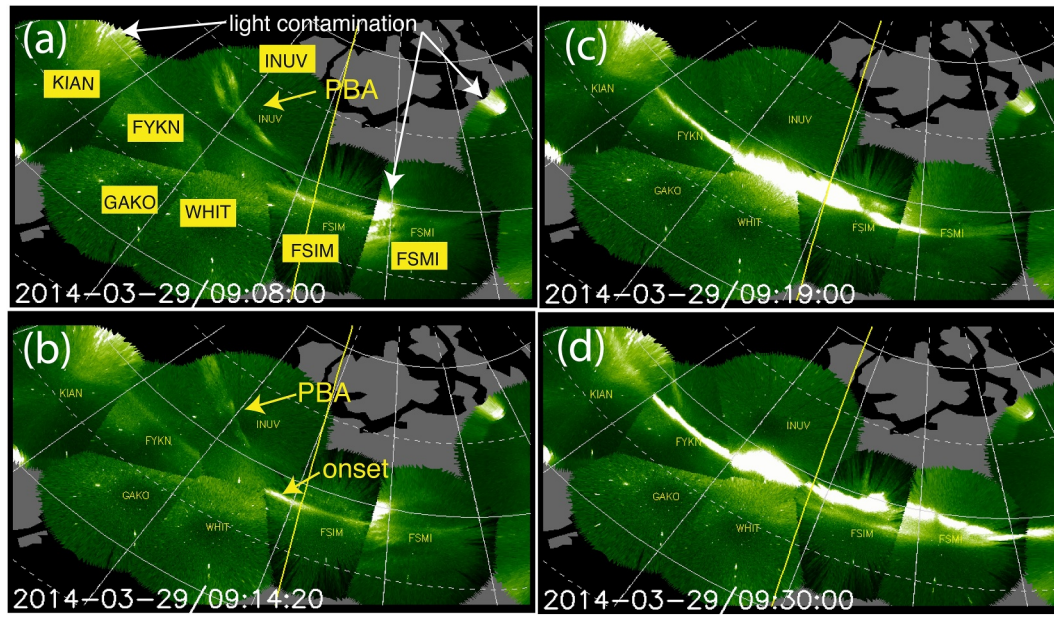

Figure 1. Selected merged images from the Time History of Events and Macroscale Interactions during Substorms all-sky-imagers (ASIs) for the period covering an auroral substorm on 29 March 2014. Yellow arrows identify auroral activities including auroral onset. Panel (a) highlight the name of ASI stations. White lines represent isocontours of magnetic latitude (every 10° in solid lines) and longitude (every 15°).

prolonged auroral streamers, whereas the third single-onset substorm consists of a sequence of PBIs and auroral streamers causing larger azimuthal and poleward expansion. For each event, we present observations from ASIs and ground magnetometers. Mosaic images from THEMIS are presented first to provide an overview of the auroral activity. Then the keograms and ground-based magnetometer observations are presented along with IMF-By/Bz and SML index to examine the auroral activities and substorm signatures in detail.

3.1. Single-Onset Substorms

3.1.1. Event 1, 29 March 2014

Figure 1 shows selected merged images from the THEMIS ASIs for the period covering a substorm on 29 March 2014. The light contamination in the images is highlighted by white arrows in Figure 1a. A movie of the merged images every 10 s is given as Movie S1. Figure 2 shows the N-S keograms of auroral intensity versus magnetic latitude, SML index, and ground magnetic field data (H-component). The last panel of Figure 2 shows the midlatitude Pi2 pulsations at a station close to the longitude of the auroral activity. The IMF-Bz turned southward at ∼09:02 UT and remained southward for the rest of the considered period. A growth-phase arc at ∼68.5° MLAT and a poleward boundary arc (PBA) were already present at the beginning of the event in the FSMI and INUV imager FOV, respectively. The PBA continuously tilted equatorward to reach close to the growth-phase arc (see Movie S1). As the tilted PBA approached the growth-phase arc near the FSIM and WHIT imager FOV, a substorm onset occurred at ∼09:14:20 UT, identified by the brightening near the western FOV of the FSIM imager at ∼68.5 MLAT near midnight. The onset was followed by the start of Pi2 pulsations at FRN. By ∼09:19 UT, the brightening expanded eastward and westward, covering FYKN and FSIM imager FOV and around ∼2 MLT wide region. The poleward expansion was ∼2° at FSIM and INUV. The stations away from the onset did not show significant poleward expansion, suggesting the smaller spatial scale of the substorm. The onset was accompanied by the maximum H drop of ∼−30 nT at FSMI, ∼−40 nT at FSIM, and ∼−15 nT at FYKN. The active onset aurora diminished after 09:30 UT, reflected in the local magnetometers and the SML index. The expansion phase of this substorm lasted for ∼15 min without additional major intensifications. Thus, this event was a single-onset substorm, not followed by a prolonged period of PBIs and streamers.

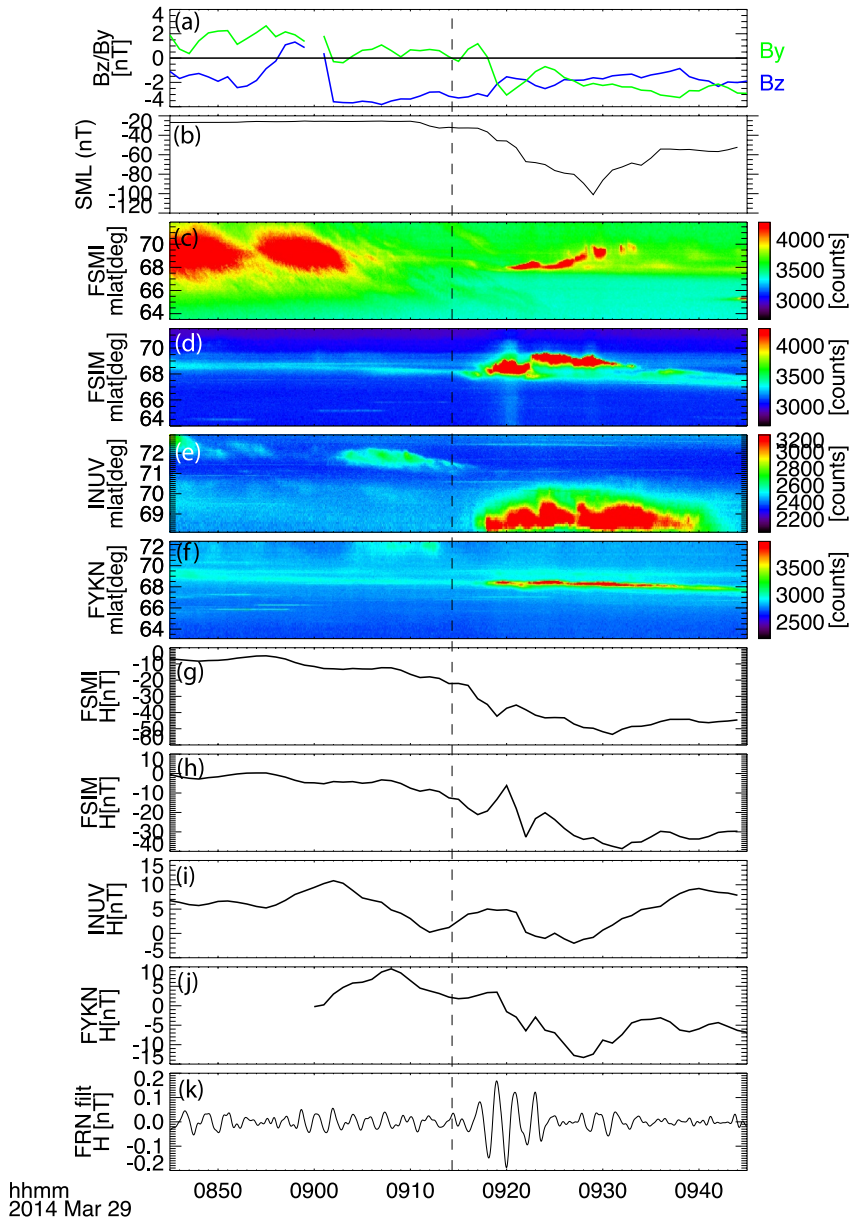

Figure 2. (a) Interplanetary magnetic field in the GSM coordinates for 29 March 2014. (b) SuperMAG SML index, (c–f) Time History of Events and Macroscale Interactions during Substorms all-sky-imager north-south keogram of FSMI, FSIM, INUV, and FYKN. (g–j) H-components magnetic field at FSMI, FSIM, INUV, and FYKN. (k) Filtered Pi2 (40–150 s passband) magnetic field data for FRN. Dashed vertical black line identifies the onset.

3.1.2. Event 2, 25 February 2008

Figure 3 shows selected merged images from the THEMIS ASIs for the period covering a substorm on 25 February 2008. A movie of the merged images every 10 s is given as Movie S2. Figure 4 shows the N-S keograms of auroral intensity versus magnetic latitude, SML index, and ground magnetic field data. The IMF-Bz was continuously southward for the time duration. The event of 25 February 2008 was originally reported by Kepko et al. (2009) and later in other substorm sequence studies (e.g., Nishimura et al., 2013; Ohtani et al., 2022). The event began with the appearance of a growth-phase arc at GILL and a pre-onset streamer, highlighted in Figure 3a. An auroral substorm onset occurred at ~05:29:30 UT, identified by the brightening and beading in the eastern FOV of the GILL imager at ~67.5° MLAT (see Figures 3b and 3c). The onset was followed by a poleward expansion of ~2.5° (as seen in the keograms in Figure 4) and associated with the Pi2 pulsations at LYFD

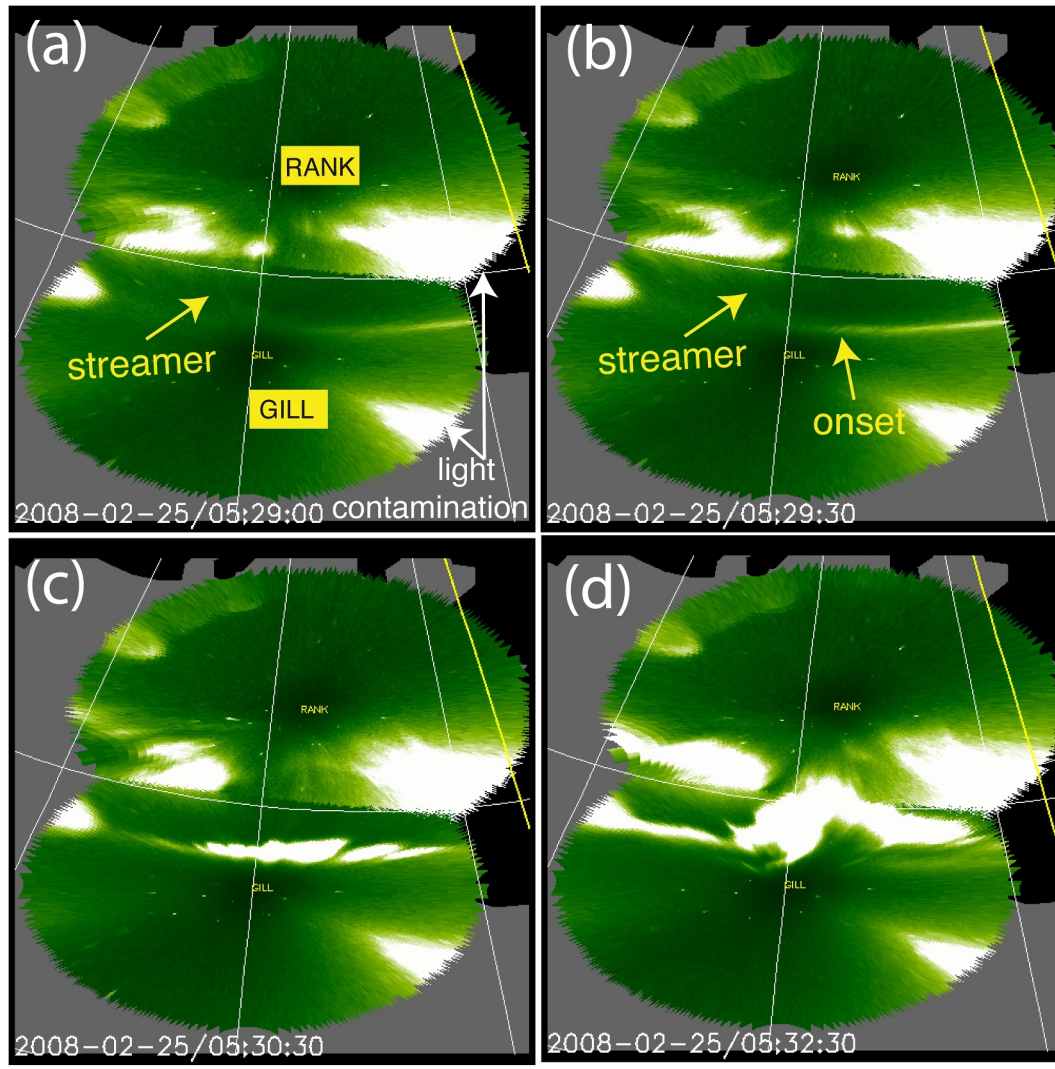

Figure 3. Selected merged images from the Time History of Events and Macroscale Interactions during Substorms all-sky-imagers (ASIs) for the period covering an auroral substorm on 25 February 2008. Yellow arrows identify the auroral activities including streamer and auroral onset. Panel (a) highlight the name of ASI stations. White lines represent isocontours of magnetic latitude (every 10° in solid lines) and longitude (every 15°).

(Figure 4h). A small decrease in H of ∼−15 nT at GILL began around 2 min before the onset, followed by a sharp positive perturbation of ∼−25 nT after the onset, suggesting the presence of eastward electrojet or positive FACs. The maximum drop was observed at SNKQ, located east of the onset. Unfortunately, due to clouds, the expansion of the aurora at SNKQ could not be observed. Although there was a decreasing trend in the SML index before the onset, the onset was associated with a sharp decrease in SML of approximately −25 nT. Thus, this event was a single-onset substorm with an expansion phase that persisted for only about 4 min.

3.1.3. Event 3, 16 February 2010

Figure 5 shows selected merged images from the THEMIS ASIs for the period covering a substorm on 16 February 2010. A movie of the merged images every 10 s is given as Movie S3. Figure 6 shows the N-S keograms of auroral intensity versus magnetic latitude, SML index, and ground magnetic field data. The IMF-Bz was consistently negative, attaining the values of ≤5 nT, throughout the considered period. The brief event in the FOV of the FSMI imager at 07:04:30 UT (Movie S3) was not followed by poleward expansion and quickly faded. We thus classify this event as pseudo-breakup, and do not consider it further.

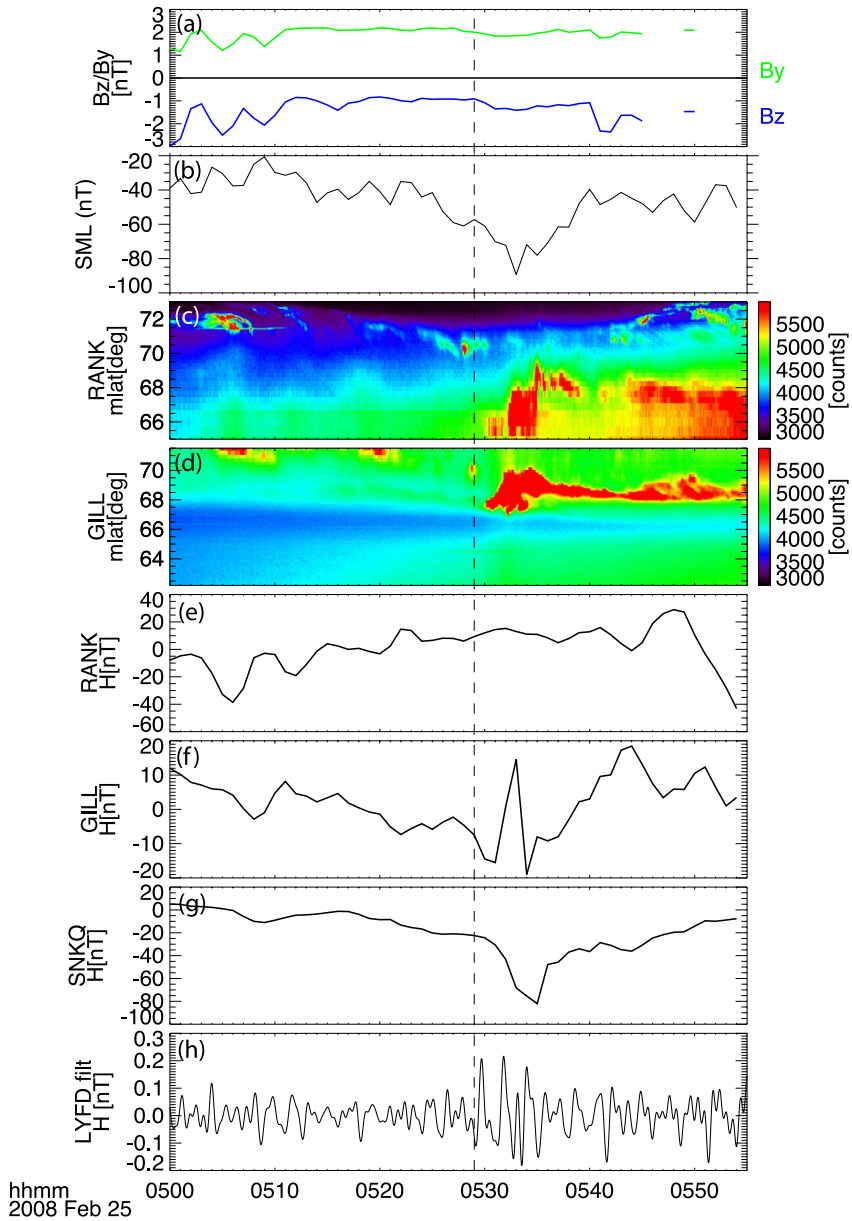

Figure 4. (a) Interplanetary magnetic field in the GSM coordinates for 25 February 2008. (b) SuperMAG SML index, (c, d) Time History of Events and Macroscale Interactions during Substorms all-sky-imager north-south keogram of RANK and GILL. (e–g) H-components magnetic field at RANK, GILL, and SNKQ. (h) Filtered Pi2 (40–150 s passband) magnetic field data for LYFD. Vertical dashed black line identifies the auroral onset.

An auroral substorm onset, characterized by an auroral brightening in the FOV of FSIM imager at ∼22.2 MLT and 65.5° MLAT, initiated at 07:17:50 UT (Figure 5a). By 07:18:50 UT (1 min after the onset; Figure 5b), the brightening rapidly expanded westward and eastward, spanning between approximately 21.7 and 23.2 MLT, and accompanied by Pi2 pulsations (Figure 6). The auroral brightening was followed by a poleward expansion. As the poleward expanding aurora reached the PBA, an abrupt poleward expansion occurred after ∼07:24 UT (∼6 min after the onset) at FSMI and FSIM followed by the streamers (Figures 5c–5e and Movie S3), associated with the second set of amplification in the Pi2 pulsations and the start of a sharp magnetic field drop at FSIM (∼−500 nT), FSMI (∼400 nT), and YKNF (∼−550 nT). The interaction of PBA with the onset aurora and the subsequent poleward expansion is clear in the FSMI and FSIM keograms (Figures 6d and 6e). By ∼07:30 UT (12 min after the onset), the aurora had expanded poleward by >5° at FSMI and FSIM, reaching >71° MLAT (see Figures 6d and 6e). The poleward expansion was followed by a prolonged period of equatorward extending streamers,

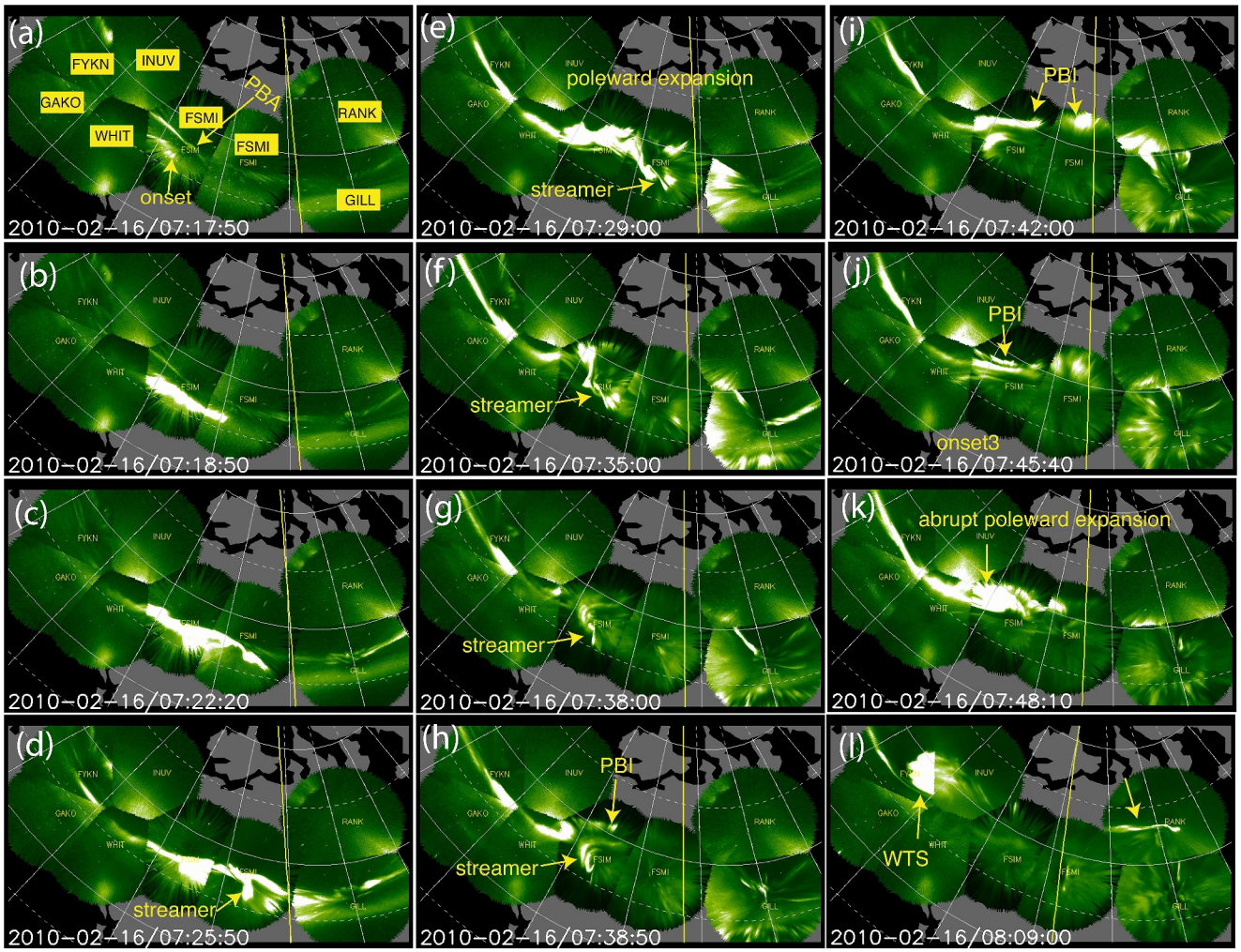

Figure 5. Selected merged images from the Time History of Events and Macroscale Interactions during Substorms all-sky-imagers (ASIs) for the period covering an auroral substorm on 16 February 2010. Yellow arrows identify the ensuing auroral activities including streamers and auroral onset. Panel (a) highlight the name of ASI stations. White lines represent isocontours of magnetic latitude (every 10° in solid lines) and longitude (every 15°).

highlighted in Figures 5d–5h. Note that the sharp drop in the SML index and local H-component began ~6 min after the auroral onset and was associated with the abrupt poleward expansion and ensuing streamers.

As the auroral intensity decreased (Figure 5g), an auroral activation began at 71° MLAT at 07:38:50 (Figure 5h), which was presumably close to the polar cap boundary and, therefore, represents a PBI, associated with the onset of the third set of Pi2 pulsations. Another auroral activation, which again may be a PBI, started at ~07:45:30 (Figure 5j) in the FSIM imager FOV, associated with the fourth set of Pi2 pulsations. Previous studies have shown that Pi2 pulsations are associated with PBIs (Kim et al., 2005; Sutcliffe & Lyons, 2002). The auroral activation associated with PBIs was followed by the poleward and azimuthal expansion and filled the upper FOV of the FSMI and FSIM imagers. The PBI extended azimuthally, and the formation of a westward expanding surge was detected in the FOV of INUV and FYKN imagers (Figures 5k and 5l). The prolonged PBI and its longitudinal extension can also be identified in the FYKN keogram (Figure 6f) as a patch of intense auroral emission. The longitudinal extension of PBIs was also reported by Ohtani et al. (2018). The PBI and subsequent auroral expansion were accompanied by the gradual drop in the magnetic field at GILL, FSMI, FSIM, and FYKN. The westward expanding surge was detected after ~08:04 UT at FYKN (Figure 5l), associated with the sudden drop of ~−50 nT at FYKN. The active aurora continued until ~08:40 UT at FYKN (Movie S3).

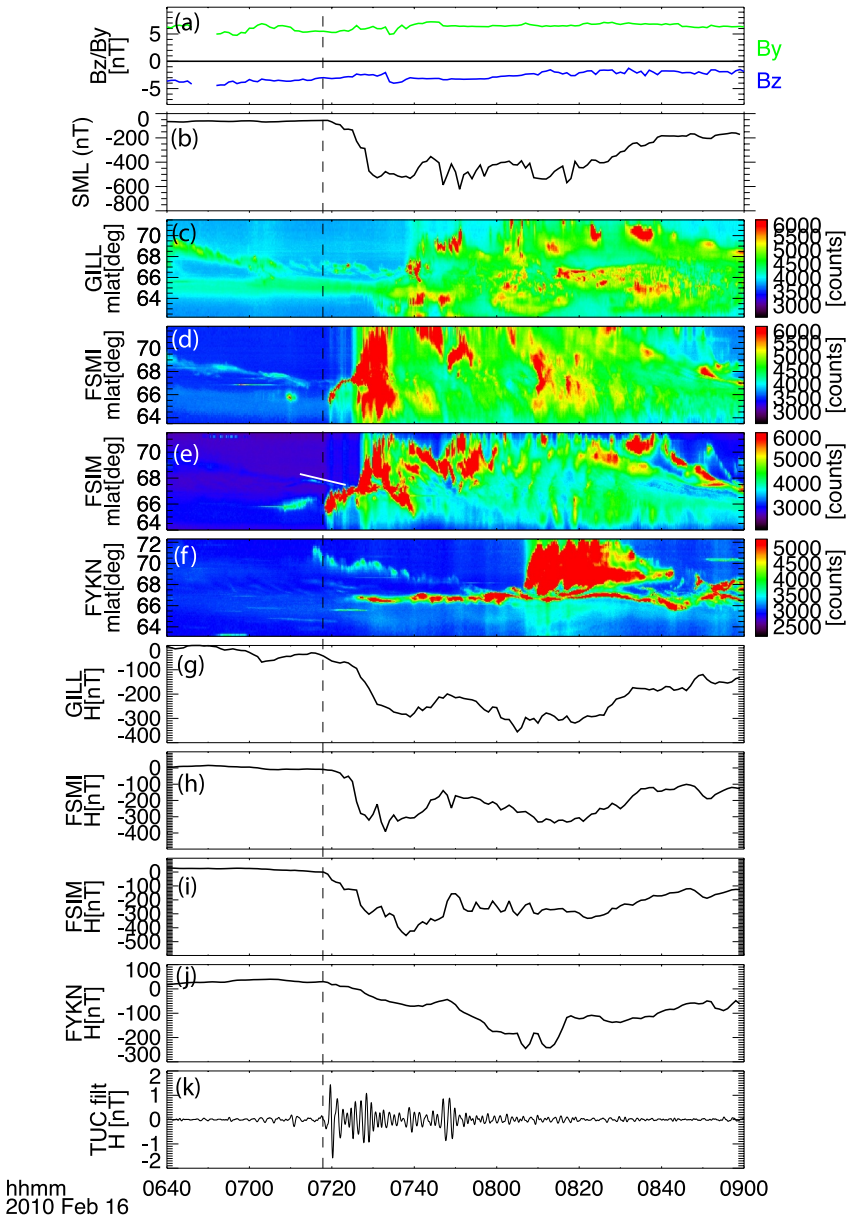

Figure 6. (a) Interplanetary magnetic field in the GSM coordinates for 16 February 2010. (b) SuperMAG SML index, (c–f) Time History of Events and Macroscale Interactions during Substorms all-sky-imager north-south keogram of GILL, FSMI, FSIM, and FYKN. (g–j) H-components magnetic field at GILL, FSMI, FSIM, and FYKN. (k) Filtered Pi2 (40–150 s passband) magnetic field data for TUC. Vertical dashed black line identifies the auroral onset.

In summary, this event shows that a single substorm onset could lead to a significant expansion of both poleward (>5°) and azimuthal (>6 MLT) extents of the active aurora and prolonged expansion phase duration. For this event, during the expansion phase of the substorm, there was an approximately 50-min-long intensification sequence along the poleward boundary (68°–72° MLAT), consisting of two discrete PBI events. After formation, the PBI extended both poleward and azimuthally, and formed a westward-expanding surge. The longitudinally extended PBI covered approximately a 3 MLT-wide region. Note that the full poleward extent of the aurora could not be determined because of the absence of imagers poleward of FSMI and FSMI. Thus, this event effectively demonstrates the role of prolonged auroral streamers and PBIs in the spatiotemporal development of the expansion phase aurora.

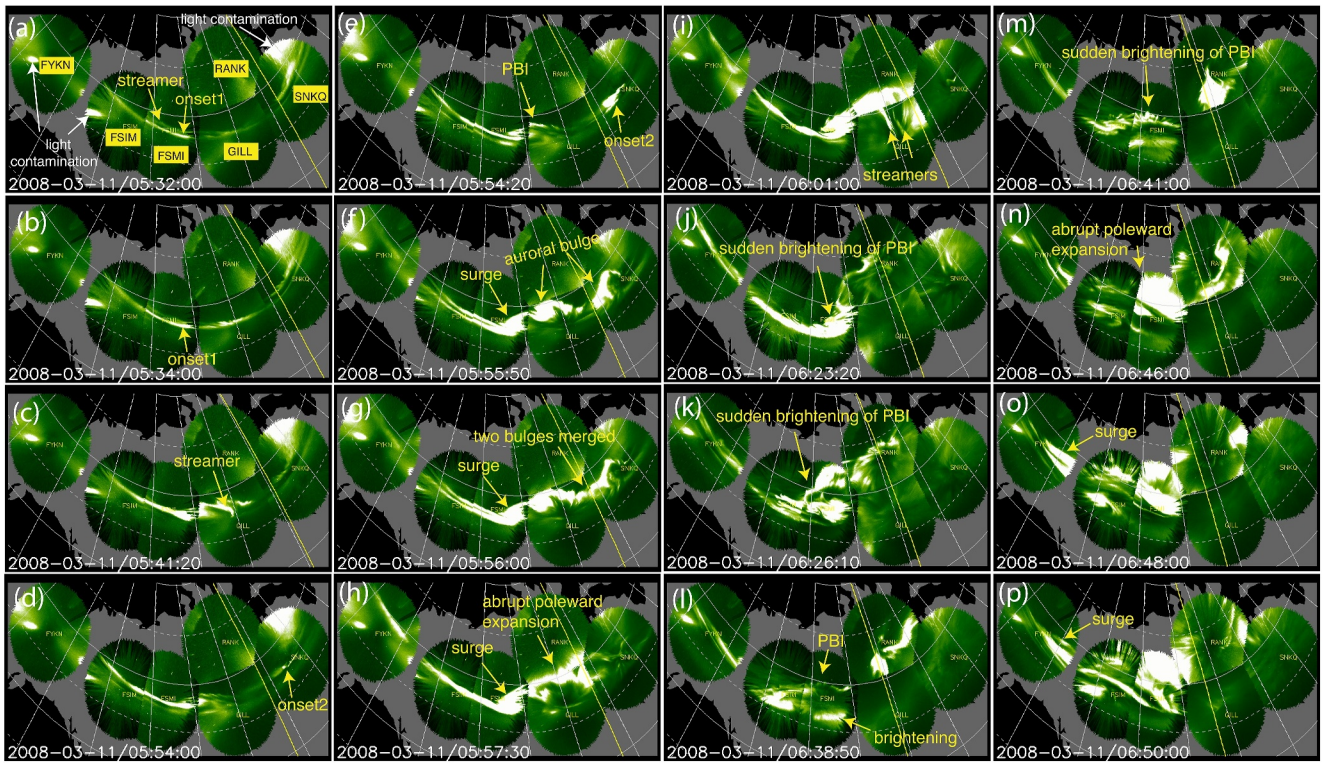

Figure 7. Selected merged images from the Time History of Events and Macroscale Interactions during Substorms all-sky-imagers (ASIs) for the period covering an auroral substorm on 11 March 2008. Yellow arrows identify the auroral activities including streamers and the auroral onset. Panel (a) highlight the name of ASI stations. White lines represent isocontours of magnetic latitude (every 10° in solid lines) and longitude (every 15°).

3.2. Multiple-Onset Substorms

3.2.1. Event 4, 11 March 2008

Figure 7 shows selected merged images from the THEMIS ASIs for the period covering a substorm on 11 March 2008. A movie of the merged images every 10 s is given as Movie S4. Figure 8 shows the N-S keograms of auroral intensity versus magnetic latitude, SML index, and ground magnetic field data. The dashed lines in Figure 8 indicate the auroral substorm onset. The IMF-Bz was slightly positive during the onset of the first substorm, turned a few nT negative at ∼05:45 UT, and maintained negative values until ∼06:45 UT. Initially, a pre-existing azimuthally extended growth phase arc appeared clearly in the FOV of the SNKQ, GILL, FSMI, and FSIM imager (Figure 7a). The brightness in the poleward FOV of the SNKQ imager is due to light contamination. The first auroral onset, identified by the brightness of the pre-existing arc in the FOV of the GILL imager, initiated around 05:32 UT at ∼23 MLT and ∼67° MLAT (Figures 7a and 7b), triggered by an eastward-tilted pre-onset streamer, indicated by an arrow in Figure 7a. This onset was followed by a localized, minor poleward expansion of ∼2.5° at GILL (see Figure 8d), and ensuing auroral streamers (Figure 7c). In association with this localized onset, no considerable disturbance was observed in the H at GILL (Figure 8h) or the SML index (Figure 8b). The Pi2 pulsations at ∼05:41 UT in Figure 8l were correlated with auroral streamers, not with the auroral substorm onset. Another strong Pi2 pulsation at ∼05:50 UT can be linked with the PBI, followed by ensuing streamer at GILL (Movie S4).

Approximately 21 min after and to the east of the previous onset, a successive auroral substorm onset occurred. This was identified by a brightening of the arc at 0.8 MLT and 67.5° MLAT in the SNKQ imager FOV, starting around 05:53 UT (Figure 7d) and identified by the second dashed line in Figure 8. Due to clouds at SNKQ, it is not clear if this auroral substorm onset was preceded by a pre-onset streamer. Simultaneously with the onset, a PBI occurred at GILL (Figure 7e) at ∼68° MLAT and 22.4 MLT, near the onset location of the previous substorm, followed by the formation of an auroral bulge. At ∼05:55:50 (Figure 7f), two bulges emerged, one at GILL at the

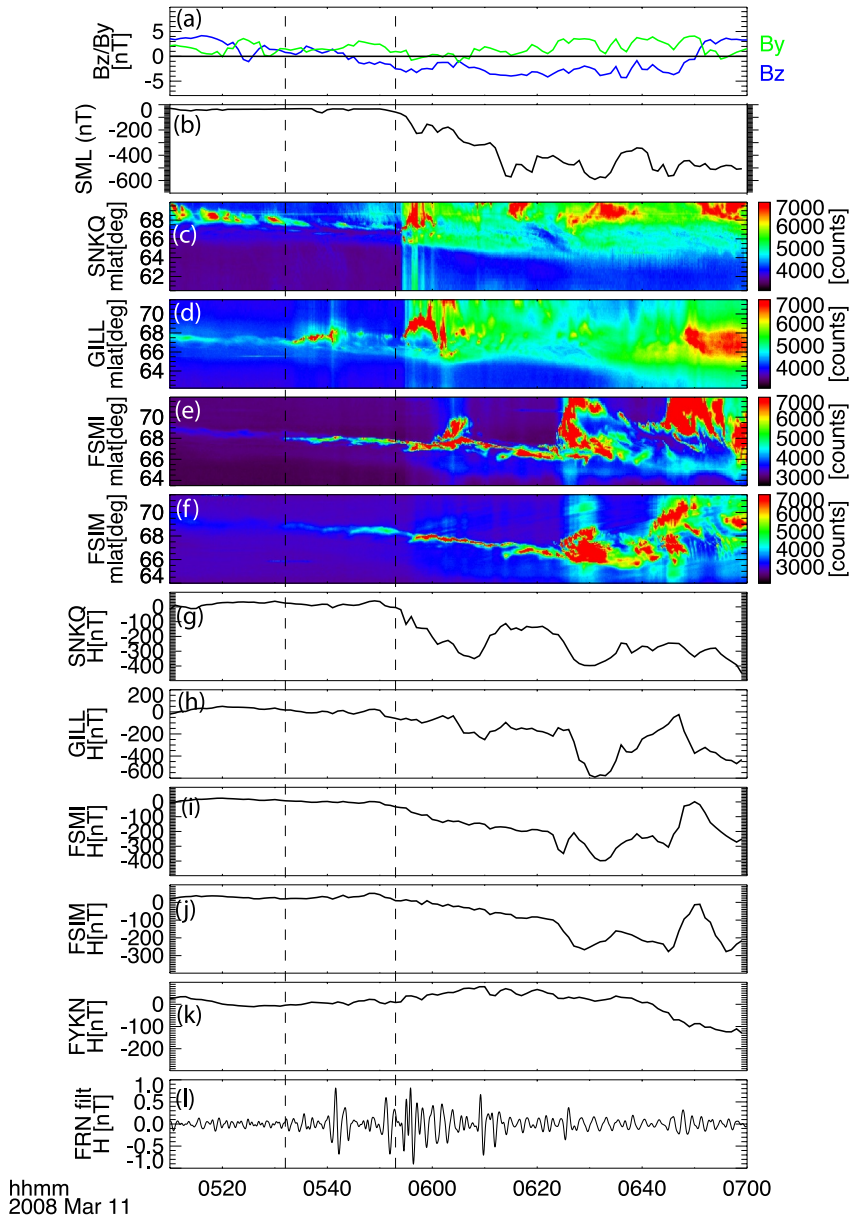

Figure 8. (a) Interplanetary magnetic field in the GSM coordinates for 11 March 2008. (b) SuperMAG SML index, (c–f) Time History of Events and Macroscale Interactions during Substorms all-sky-imager north-south keogram of SNKQ, GILL, FSMI, and FSIM. (g–k) H-components magnetic field at SNKQ, GILL, FSMI, and FSIM. (l) Filtered Pi2 (40–150 s passband) magnetic field data for FRN. Vertical dashed black lines identify the auroral onset.

location of the initial onset and the other at SNKQ related to the successive onset. Subsequently, the two bulges merged, resulting in a significantly spread active aurora, spanning approximately 4 MLT with a poleward expansion of >3° at GILL (see Figures 7h and 8d and Movie S4). This led to a surge detected at FSMI, highlighted in Figures 7f and 7g. After that, several streamers emerged out from the poleward boundary of the auroral oval, apparent primarily in the GILL imager FOV (Figure 7i), associated with Pi2 pulsations and a drop of ∼−200 nT in H at GILL (Figure 8h). The amplification of Pi2 pulsations at ∼06:09 UT may be associated with the PBI, evident in the FOV of the SNKQ imager (Movie S4).

As the recovery phase of the previous substorm was in progress, abrupt brightening occurred at 06:23:20 UT in the FSMI imager FOV at 67.5° MLAT and 22.3 MLT (Figure 7j). Since this brightening occurred along the poleward boundary, it is more likely to be a PBI intensification rather than a successive onset. After that the aurora

reached its highest latitude of >∼72° MLAT within 2 min (Figures 7k and 8e). The PBI and abrupt poleward expansion was accompanied by a third-step decrease in the SML index of ∼−200 nT, and a notable decrease in the local magnetometers.

Another brightening began at 06:38:50 UT along the auroral poleward boundary in the FSMI imager FOV (22.4 MLT and 66° MLAT). The brightened arc gradually diminished without any subsequent auroral breakup. However, during this fading period, a sudden brightening of the PBI occurred around 06:41 UT (Figure 7m), followed by a rapid and abrupt poleward expansion (poleward explosion) starting from around 06:44 UT (Figure 7n and Movie S4). This expansion extended across the upper FOV of FSMI and FSIM imagers (Figures 7n–7p, 8e and 8f). Due to the absence of imagers poleward of FSMI, it is not possible to ascertain the poleward extent of the active aurora. The sudden poleward expansion coincided with the sharp positive perturbation (of ∼250–300 nT) at FSMI and FSIM, indicating intensification of the eastward electrojet or positive FACs equatorward of the brightening. Therefore, the new auroral activation coincided with the sudden brightening and poleward explosion of the PBI. Following this activity, the auroral surge was detected in the eastern FOV of the FYKN imager (Figure 7o), also evident by the onset of the negative bay at FYKN. The auroral activation due to PBIs persisted for ∼20 min (keograms and Movie S4), covering a longitudinal region ∼3 MLT wide. Thus, the further azimuthal (>5 MLT) and poleward expansion of the active aurora was associated with the longitudinal extension of PBI, not with the new subsequent auroral onset. The fourth-step decrease of ∼−200 nT in the SML index coincided with the onset of PBI at ∼06:41 UT.

In summary, this event illustrates that the sudden intensification of the poleward boundary, followed by poleward explosion and westward expansion, can further contribute to the expansion of the active aurora. It's worth noting that relying solely on magnetometer data, the event of a long brightening sequence of PBI followed by an abrupt poleward expansion might be mistaken for a new successive onset. The two successive onsets followed by two events of long intensification sequence of the poleward boundary, which also consists of poleward explosion of the active aurora, led to prolonged expansion phase activity lasting for 1 hr, covering a wide MLT region of over 6 hr and poleward expansion of >5°. The successive onsets and prolonged PBIs were accompanied with stepwise development of the SML index.

3.2.2. Event 5, 02 February 2008

Figure 9 shows selected merged images from the THEMIS ASIs for the period covering a substorm on 02 February 2008. A movie of the merged images every 10 s is given as Movie S5. Figure 10 shows the N-S keograms of auroral intensity versus magnetic latitude, SML index, and ground magnetic field data. The dashed lines in Figure 10 indicate the auroral substorm and successive auroral onsets. The IMF-Bz fluctuated between northward and southward orientations throughout the considered time and exhibited a southward turn before all the auroral onsets. The event begins with the appearance of a bright growth-phase arc, prominently visible within the FSMI and GILL imager FOV, alongside an eastward tilted pre-onset streamer at GILL, indicated by an arrow in Figure 9a. The substorm auroral onset, characterized by the brightening of pre-existing arc, initiated at ∼07:38:50 UT (∼0.5 MLT and ∼65° MLAT) near the western FOV of the GILL imager. The brightened onset arc expanded westward, reaching the FOV of GAKO by around 07:44 UT (5 min after the onset; Figure 9b), covering ∼4 MLT. The onset is followed by the poleward expansion of ∼3° at GILL and ∼2° at FSMI and FSIM (Figure 10). The onset was soon followed a sharp H bay at GILL of ∼−250 nT, ∼−150–200 nT at FSMI and FSIM, and ∼−100 nT in the SML index, associated with the onset of auroral poleward expansion and activity within the bulge.

As the auroral activity began to diminish, a successive auroral onset, evident by the brightening near the eastward edge of the FSMI imager FOV, initiated at ∼07:57:30 UT (∼0.3 MLT and ∼65.5° MLAT), westward of the previous onset (Figures 9c and 9d). Occurring 19 min after the first onset, this successive onset appeared to be triggered by the westward tilted PBA, taking the form of a streamer (see Movie S5). The streamer persisted even after the onset and appeared to pull the onset aurora poleward, forming a small auroral bulge (Figure 9e), apparent near the eastern edge of the FSMI imager FOV. The bulge exhibited no westward propagation and, therefore, is not observable in the FSMI keogram because the keogram is made by slicing the images at the central meridian. This successive onset did not cause considerable poleward expansion and was relatively localized, resulting in auroral intensification primarily within the FSMI and GILL imager FOV, covering ∼2.5 MLT region.

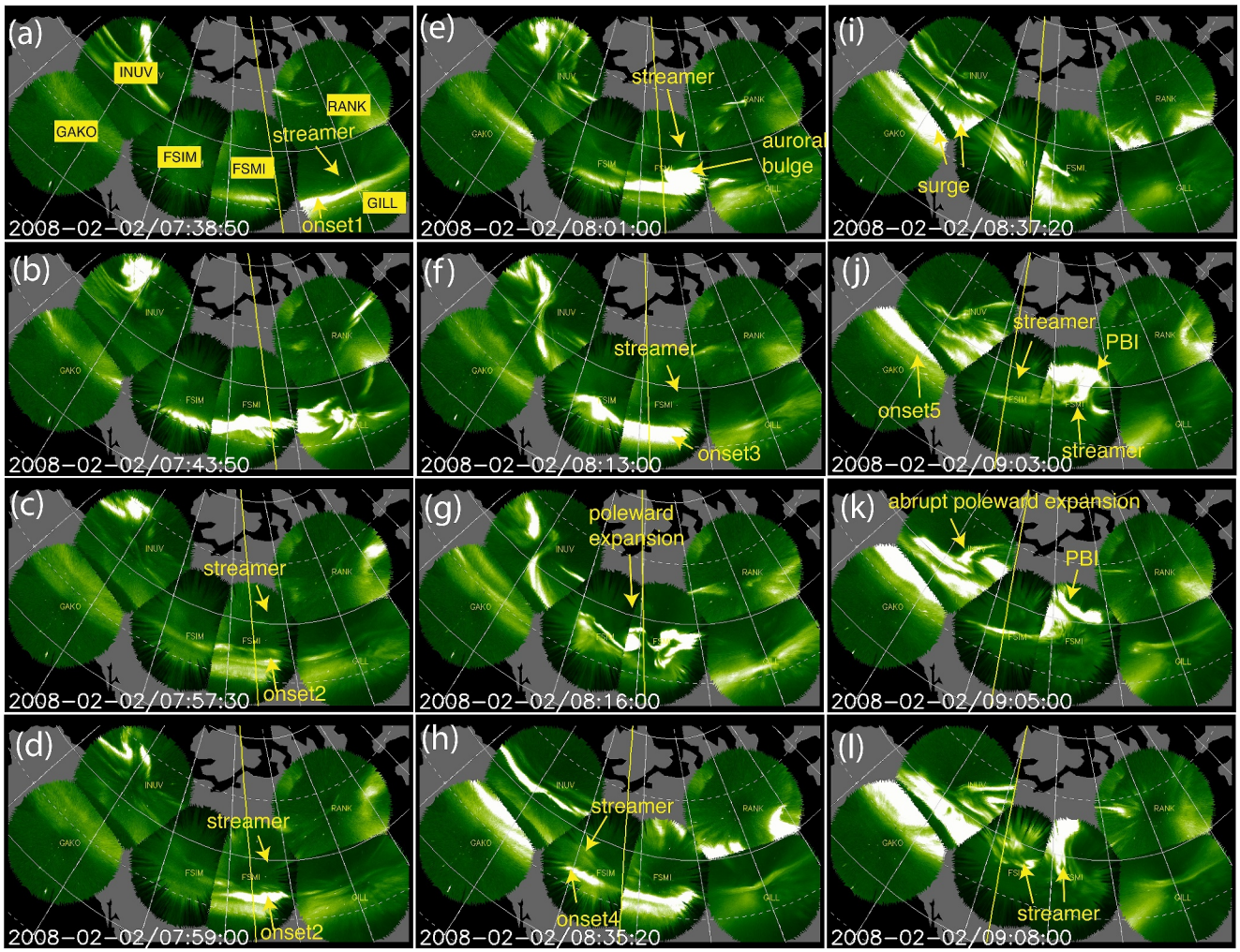

Figure 9. Selected merged images from the Time History of Events and Macroscale Interactions during Substorms all-sky-imagers (ASIs) for the period covering an auroral substorm on 02 February 2008. Yellow arrows identify the streamers, poleward boundary arc, and ensuing auroral activities including the auroral onset. Panel (a) highlight the name of ASI stations. White lines represent isocontours of magnetic latitude (every 10° in solid lines) and longitude (every 15°).

Consequently, the H showed a drop at GILL (∼−150 nT), FSMI (∼−30 nT), and the SML index showed a second-step drop of ∼−100 nT.

While the expansion phase of the previous substorm onset was in progress, a new successive onset was initiated at ∼08:13 UT (∼00 MLT and ∼65.5° MLAT), evident as a brightening of the arc at FSMI, highlighted in Figure 9f. The new successive onset initiated equatorward of the post-onset streamer, highlighted by an arrow in Figure 9f. Occurring 15 min after the previous onset, the new onset was followed by an abrupt poleward expansion at FSIM and FSMI (Movie S5). The aurora reached its highest latitude of ∼69° at ∼08:16 UT, 3 min after the onset (Figure 10). This caused an abrupt decrease of ∼450 nT at FSMI and ∼−300 nT at FSIM and a third-step decrease of ∼200 nT in the SML index (Figure 10).

As the auroral activity from the earlier successive auroral onset decreased, another successive onset, identified by the brightening of arc within the FOV of the FSIM imager, began at 08:35 UT (23.5 MLT and ∼66° MLAT), westward of the previous onset (Figure 9h) and 23 min after the previous onset. Like the previous onsets, this onset was also initiated by the post-onset streamer, highlighted by an arrow in the FOV of the FSIM imager (Figure 9h). The onset was followed by the poleward expansion, ensuing streamers, and the formation of the surge, which reached INUV and GAKO imagers FOV by 08:37 UT (Figure 9i). The aurora reached its highest latitude of >71° MLAT within 1 min after the onset. This leads to a sharp decrease of ∼−300 nT at FSIM and a

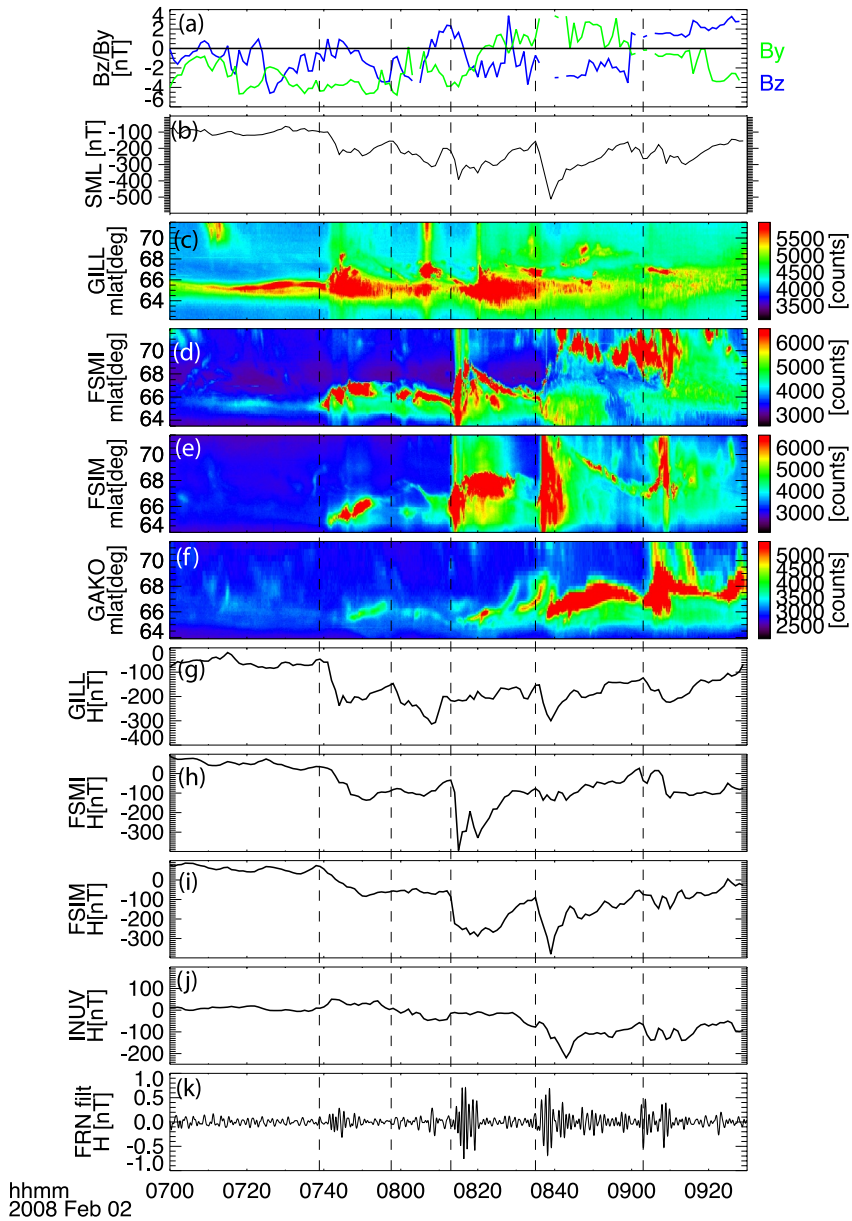

Figure 10. (a) Interplanetary magnetic field in the GSM coordinates for 02 February 2008. (b) SuperMAG SML index, (c–f) Time History of Events and Macroscale Interactions during Substorms all-sky-imager north-south keogram of GILL, FSMI, FSIM, and GAKO. (g–j) H-components magnetic field at GILL, FSMI, FSIM, and INUV. (k) Filtered Pi2 (40–150 s passband) magnetic field data for FRN. Vertical dashed black line identifies the auroral onset.

corresponding drop in the SML index (Figure 10). The active aurora from the new successive onset merged with the aurora from the previous onset, causing the azimuthal expansion of >4 MLT.

From 08:40 to 09:10 UT, within the FOV of the FSMI imager (Figures 9j and 9k), a 30-min-long intensification sequence occurred along the poleward boundary (>67° MLAT), consisting of multiple episodes of PBI, accompanied by Pi2 pulsations during this period (Figure 10j). Then, another successive onset, characterized by the brightening in the FOV of the GAKO imager, occurred at 09:03 UT (~22.7 MLT and >~66.5° MLAT), westward of the previous onset and 28 min after the earlier onset. It is not clear if a streamer triggered this onset due to the already bright aurora just poleward of the onset. The onset aurora reached its highest latitude of >~71° MLAT within 2 min after the onset (Figures 9k and 10f). The aurora from the new onset merged with that from the previous one, further expanding the active aurora azimuthally (as evidenced by the intensification of aurora at

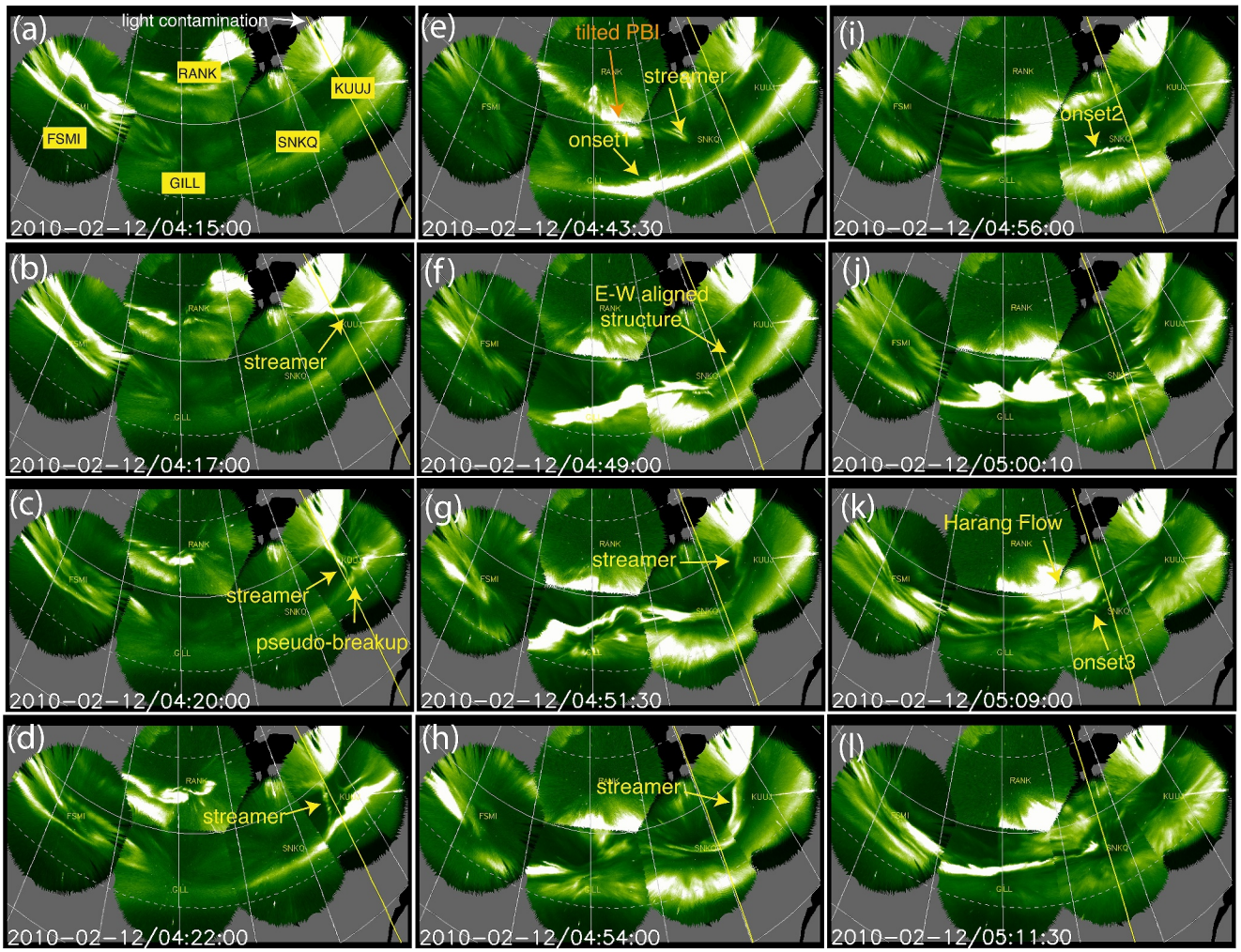

Figure 11. Selected merged images from the Time History of Events and Macroscale Interactions during Substorms all-sky-imagers (ASIs) for the period covering an auroral substorm on 12 February 2010. Yellow arrows identify the auroral activities including the auroral onset and streamers. Panel (a) highlight the name of ASI stations. White lines represent isocontours of magnetic latitude (every 10° in solid lines) and longitude (every 15°).

INUV and GAKO), thereby extending the expansion phase aurora to cover a region wider than 5 MLT. The onset was followed by a decrease of ∼−100 nT in the SML index. Unfortunately, the H data at GAKO was unavailable for this event. The strong Pi2 pulsations after the onset at ∼09:06–09:08 were associated with the auroral streamers observed at FSIM and FSMI (Figure 9l).

In summary, five successive onsets occurred within a span of 90 min. Each onset occurred westward and poleward of the previous one, except for one that occurred equatorward of the preceding onset. All onsets were accompanied by Pi2 pulsations and intensification of the SML index. This systematic westward and poleward occurrence of successive onsets led to the stepwise westward and poleward expansion of the onset aurora. The aurora from the new onsets merged with that from the previous onset, furthering the westward expansion of the active aurora. These successive westward-occurring onsets fed the westward and poleward expansion of auroral activity, resulting in the active aurora over a >5 hr MLT wide region for approximately 1.5 hr with the maximum poleward extent of >6°. Furthermore, a prolonged (∼30 min) sequence of PBIs contributes to the poleward expansion of the aurora in addition to successive onsets.

3.2.3. Event 6, 12 February 2010

Figure 11 presents the selected snapshots of the merged images from THEMIS ASIs showing the auroral activity for the event on 12 February 2010. A movie of the merged images at every 10s is given as Movie S6.

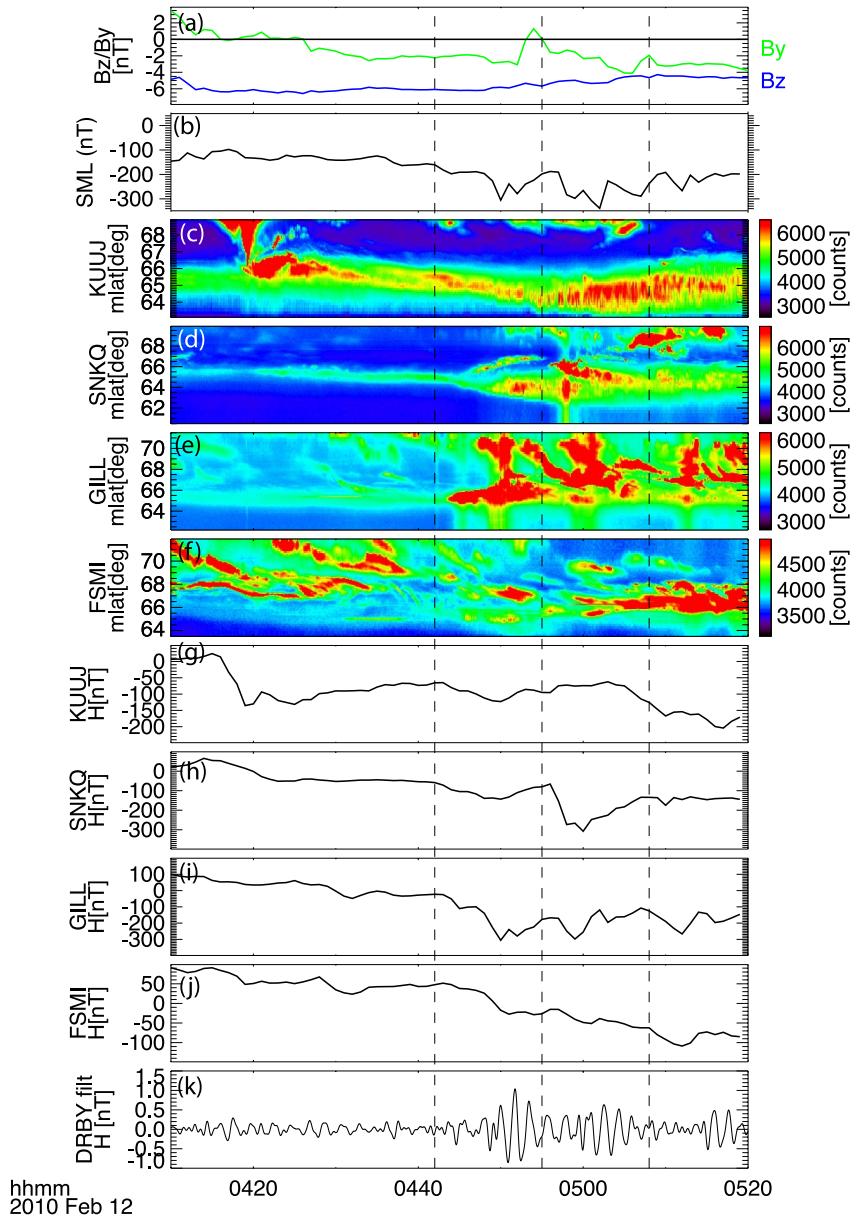

Figure 12. (a) Interplanetary magnetic field in the GSM coordinates for 12 February 2010. (b) SuperMAG SML index, (c–f) Time History of Events and Macroscale Interactions during Substorms all-sky-imager north-south keogram of GILL, FSMI, and FSIM. (g–j) H-components magnetic field at GILL, FSMI, and FSIM. (k) Filtered Pi2 (40–150 s passband) magnetic field data for DRBY. Vertical dashed black line identifies the auroral onset.

Figure 12 shows the N-S keograms of auroral intensity at KUUJ, SNKQ, GILL, and FSMI along with the H magnetic field variation, Pi2 pulsations, IMF By/Bz, and SML index. The IMF-Bz remained consistently negative throughout the entire duration under consideration. Initially, a pre-existing azimuthally extended growth phase arc appeared in the KUUJ, SNKQ, and GILL imager FOV (Figure 11a). The brightness in the poleward side of the KUUJ imager FOV is light contamination. Despite the light contamination, a bright, equatorward, and westward propagating streamer (Figure 11b) emerged from the poleward side of the KUUJ imager after ~04:15 UT. This streamer can be identified as a bright V-shaped structure in the KUUJ keogram. As this streamer touched the growth phase arc, it triggered a pseudo-breakup at the meridian of the streamer at 00 MLT (66.5° MLAT) and ~04:19 UT (Figure 11c). The bright incident streamer remained connected with the active aurora even after the breakup (Figure 11d and Movie S6). This localized activity was accompanied by a poleward expansion of ~1.5° at KUUJ. The onset of negative bay of ~−150 nT at KUUJ and SNKQ of

∼−100 nT, and Pi2 pulsation at KUUJ coincided with the onset of streamer at ∼04:15 UT, not with the onset of pseudo-breakup.

Between 04:27 and 04:34 UT, a bright streamer emerged from the PBI occurred along the westward boundary of the RANK ASI FOV. The streamer transitioned into the GILL ASI FOV without initiating any new auroral activity, consistent with the expectation that not all streamers lead to new onset. Another PBI started to occur in the RANK ASI FOV at ∼04:36 UT. The PBI tilted southwest, and a streamer began to appear clearly at the eastern portion of the tilted PBI from 04:40 UT. As this streamer (highlighted by an arrow in Figure 11e) transition from the RANK to SNKQ imager FOV and came close to the growth phase arc, an auroral onset triggered at 04:42 UT (∼22.7 MLT and 65° MLAT) near the western/eastern edge of the SNKQ/GILL imager FOV (Figure 11e). Around 10 min after the onset, the active aurora reached its highest latitude of >∼70° MLAT (>5°), with the azimuthal extent of ∼3 MLT (Figures 11g and 12e). This auroral substorm onset was followed by the mid-latitude Pi2 pulsations, start of a sharp negative bay of ∼300 nT at GILL, −60 nT at SNKQ, and −120 nT in the SML index in association with the ensuing auroral expansion.

While the expansion phase from the above onset was in progress, an east-west aligned auroral structure appeared covering the FOV of SNKQ and KUUJ imager at ∼04:49 UT (Figure 11f). By ∼04:51 UT, an equatorward propagating, westward tilted auroral streamer (Figure 11g) emerged from the poleward FOV of the KUUJ imager and merged with the east-west aligned auroral structure (Movie S6). Immediately equatorward of the westward edge of the east-west aligned portion of auroral streamer, a successive substorm auroral onset initiated in the SNKQ imager FOV at ∼04:55 UT (∼23.6 MLT and 66° MLAT), 13 min after and to the east of previous substorm onset (Figure 11i). The subsequent expansion phase aurora rapidly expanded in both the eastward and westward directions (evident from the intensified auroral activity observed in the keogram at KUUJ, SNKQ, and GILL (Figure 12)), spanning an azimuthal extent of approximately 4 MLT. The successive onset was accompanied by an abrupt decrease in H at SNKQ (∼250 nT), GILL (∼100 nT), and −150 nT in SML index. Note that high-amplitude Pi2 pulsations started at ∼04:49 UT, before the onset, coincided with the onset of streamer at KUUJ.

Close to midnight, after ∼05:04 UT, a bright auroral structure appeared in the poleward FOV of the SNKQ and GILL imager and equatorward FOV of RANK imager (Movie S6). The poleward and equatorward portion of this structure turned eastward and westward, respectively, leading to the formation of clockwise rotated structure (Harang aurora). A new longitudinally expanded (∼3 MLT wide) brightening of the arc occurred immediately equatorward of this clockwise rotated streamer in the SNKQ imager FOV at ∼05:09 UT (67° MLAT) (Figure 11k), 14 min after the previous substorm onset. As this brightening appeared nearly simultaneously across a broad longitudinal range, we construed it as the initial brightening, which is used to mark the auroral onset. The onset is followed by the poleward expansion of ∼3.5° at GILL within ∼4 min of the onset. The new successive onset further fed the ongoing expansion phase and cased a westward expansion of the active aurora, which can be identified by the enhanced aurora at FSMI (Figure 12f). The new successive onset was followed by a decrease of ∼−100 and ∼−60 nT in the H component at GILL and FSMI, respectively, as well as perturbations in the SML index of ∼−50 nT.

In summary, this event effectively illustrates the role of post-onset streamers in triggering successive onsets, both westward and eastward of the initial auroral substorm onset, resulting in spatial expansion in both directions. Additionally, the new onsets occurred poleward of the previous one, contributing to further poleward expansion of the active aurora. As a result of the successive onsets, the active aurora persisted for approximately 40 min, spanning an approximate 4.5 MLT range.

3.2.4. Event 7, 21 March 2015

Figure 13 presents the selected snapshots of the merged images from THEMIS ASIs showing the auroral activity for the event on 21 March 2015. A movie of the merged images at every 10s is given as Movie S7. Figure 14 shows the N-S keograms of auroral intensity at GILL, FSMI, FSIM, and FYKN along with the H magnetic field variation, Pi2 pulsations, IMF By/Bz, and SML index. Unfortunately, the H data at FSIM was unavailable for this event. The event begins with the occurrence of a pseudo-breakup at GILL at ∼06:18 UT (Figure 13a), characterized by beading followed by no considerable poleward expansion. As the brightness associated with the pseudo-break decreased, an auroral substorm onset, identified by the brightness and subsequent beading at ∼64° MLAT and 22.3 MLT, initiated at around 06:23:20 UT (Figure 13b) in the FSMI imager FOV. Within 1.5 min after the onset, the brightening expanded to cover ∼2 MLT wide region and expanded poleward by ∼1°

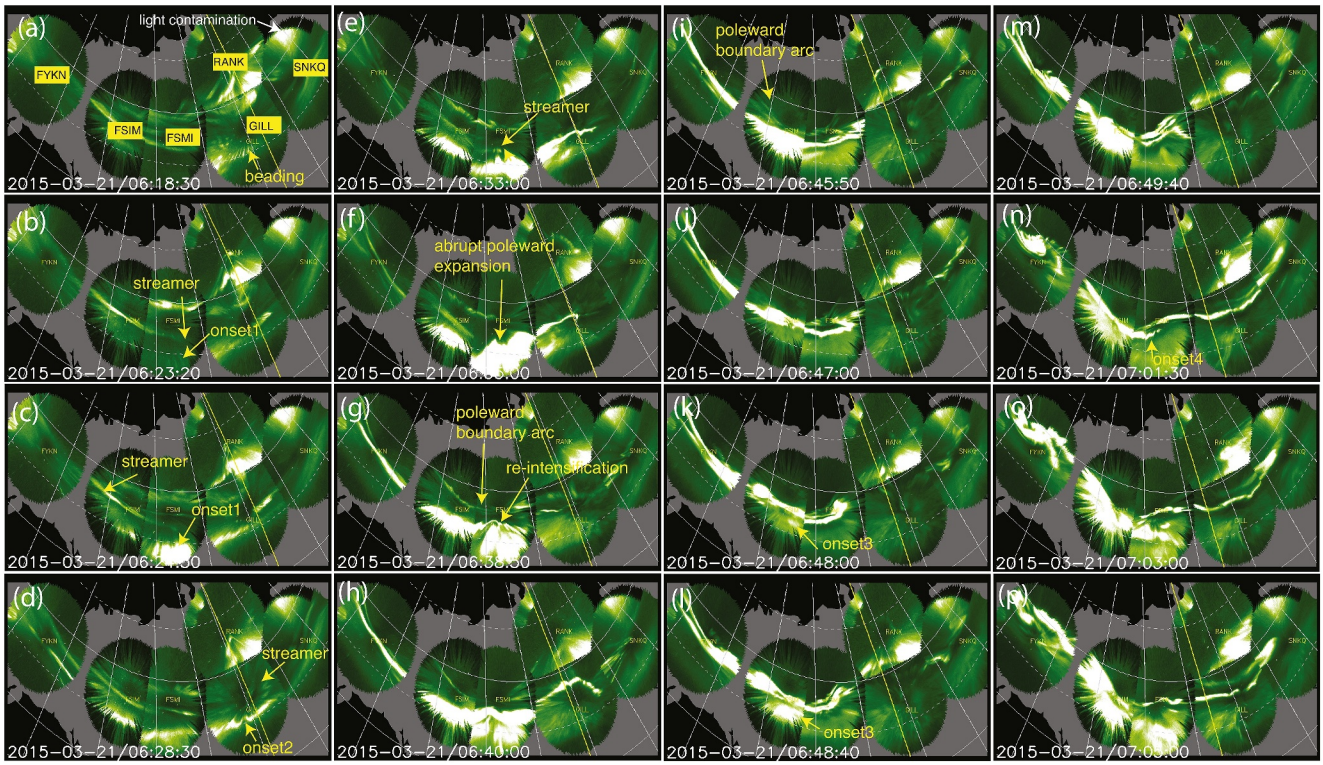

Figure 13. Selected merged images from the Time History of Events and Macroscale Interactions during Substorms all-sky-imagers (ASIs) for the period covering an auroral substorm on 21 March 2015. Yellow arrows identify the streamers and auroral activities including the auroral onset. Panel (a) highlight the name of ASI stations. White lines represent isocontours of magnetic latitude (every 10° in solid lines) and longitude (every 15°).

(Figures 13c and 14d). The onset, which occurred immediately equatorward of the eastern portion of the azimuthally extended streamer (highlighted by an arrow in Figure 13b), was not associated with any considerable H response (Figure 14).

Again, as the auroral activity at FSIM began to reduce, a successive substorm auroral onset, identified by the brightening in the FOV of GILL imager at ∼23.8 MLT and ∼64° MLAT, initiated at ∼06:28:20 UT (5 min after the previous onset; Figure 13d). Occurring east of the previous onset, the new successive onset at GILL appeared to be triggered by the post-onset streamer, highlighted by an arrow in Figure 13d. The brightening arc rapidly expanded and merged with the aurora of the previous onset in the west, causing the brightened arc to cover a 3 MLT region just 1 min afterward. The brightening was followed by poleward expansion, which intensified at FSMI after 06:33 UT when an east-west aligned streamer, which seemingly detached from the PBA, contacted the bulge, clearly seen in the FSMI keogram (highlighted by a white solid line Figures 13e, 13f, and 14d, and Movie S7). This caused a poleward expansion of ∼3° at GILL and ∼1.5° FSMI (see keograms). The successive onset was accompanied by the H decrease at FSMI (∼−50 nT) and GILL (∼−100 nT) and start of negative bay in SML index. Thus, two substorm auroral onsets occurred within a span of ∼10 min within 10° longitude, each associated with Pi2 pulsations and poleward expansion.

At ∼06:38:50 UT (∼10 min after onset2), an abrupt auroral intensification extending eastward began at the poleward boundary of the active auroral bulge in the FSMI imager FOV (Figures 13g and 13h and Movie S7). Since this intensification occurred on the same arc and was not separated from the prevailing bulge, we believe it may represent the re-intensification of the previous onset. Interestingly, this re-intensification occurred immediately equatorward of the PBA, highlighted by an arrow in Figure 13g. The equatorward propagating PBA and re-intensification of the existing bulge is clear in the FSMI keogram (Figure 14d, second white line). These activities resulted in further poleward expansion of the active aurora at GILL, FSMI, and FSIM (Figures 14c–14e and Movie S7). This successive onset was accompanied by the negative H-response at FSMI (−200 nT) and GLL (∼−50 nT).

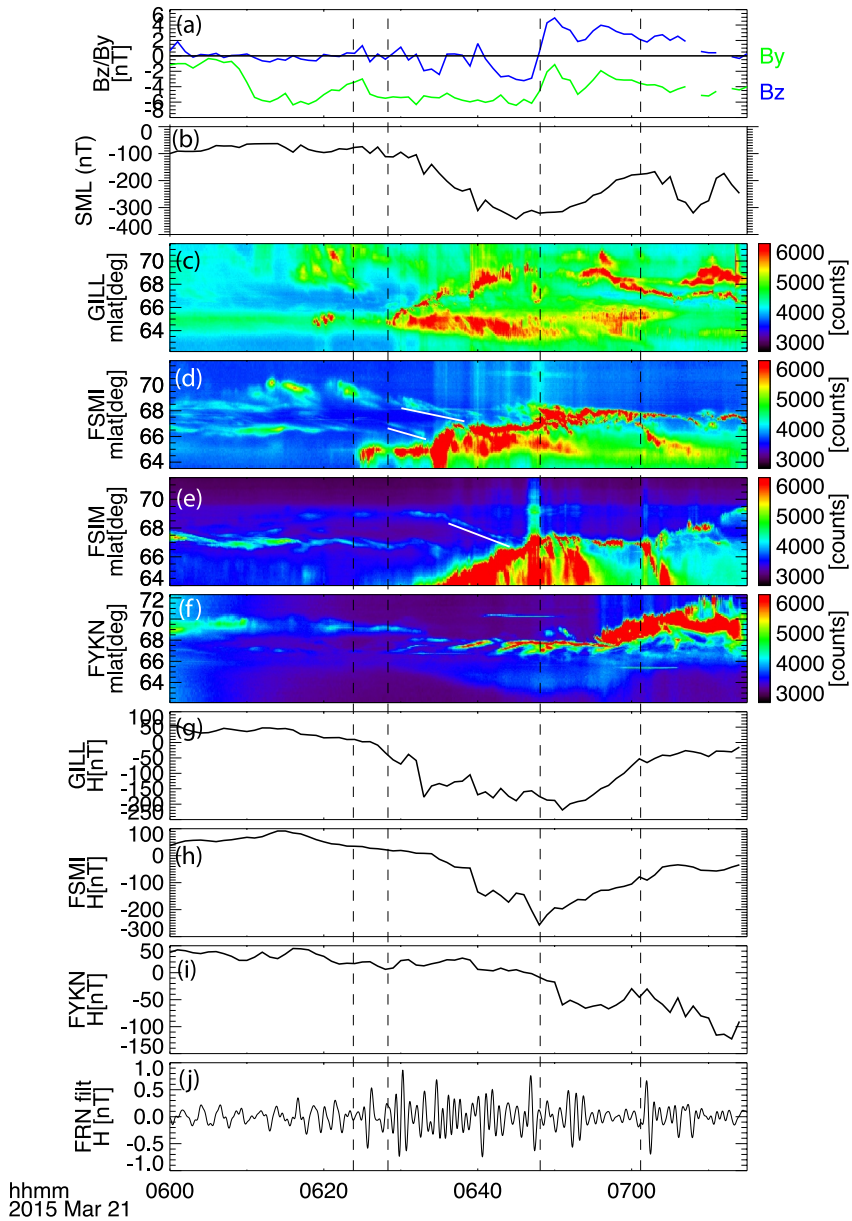

Figure 14. (a) Interplanetary magnetic field in the GSM coordinates for 21 March 2015. (b) SuperMAG SML index, (c–f) Time History of Events and Macroscale Interactions during Substorms all-sky-imager north-south keogram of GILL, FSMI, FSIM, and FYKN. (g–i) H-components magnetic field at GILL, FSMI, and FYKN. (j) Filtered Pi2 (40–150 s passband) magnetic field data for FRN. Solid vertical black line identifies the auroral onset. The equatorward motion of poleward boundary arc is highlighted by solid white lines.

At ∼06:48 UT, a new successive auroral substorm onset occurred in the FSIM imager FOV at ∼66° MLAT and 21.9 MLAT. Interestingly, this onset occurred after the continuously equatorward propagating PBA merged with the active aurora (Movie S7). The interaction of equatorward moving PBA and aurora can be clearly seen in the keogram at FSIM (highlighted by white line in Figure 14e). Occurring equatorward of the previous subsequent onset and associated with Pi2 pulsations, the onset aurora of the new successive onset merged with the aurora from the previous onset, causing the further intensification of the active aurora (Figures 13l and 13m).

While the active aurora from the previous substorm onsets was persisting, another successive onset, identified by the brightening and beading in the FOV of FSMI at ∼67° MLAT and 23 MLT, initiated at ∼07:01:30 UT, eastward of the previous onset (Figure 13n). Occurring ∼16 min after the previous onset, this onset caused further

azimuthal and expansion of the active aurora, evident by the intensification of the active aurora at GILL, FSMI, FSIM, and FYKN (Figures 13o, 13p, and 14). The recurring PBIs were also observed in the FOV of FYKN and RANK imager after the onset.

In summary, this event effectively illustrates how successive onsets influence both the azimuthal (both eastward and westward) and poleward extent of the expansion phase aurora, as well as its duration. Apart from the auroral substorm onsets, this event also showed auroral re-intensifications (re-intensification of the previous onset), likely triggered by flow channels associated with the PBA (Lyons, Liu, Nishimura, Wang, et al., 2021). The observations indicate that auroral re-intensifications occurred when the PBA approached the expansion phase aurora. These findings suggest that flow channels associated with PBAs may supply new plasma to the auroral surge, leading to further auroral re-intensifications. It is interesting to note the stepwise poleward expansion of the active aurora due to auroral substorm onsets and auroral re-intensifications, clearly observed in the FSMI keogram (Figure 14d). As a result of four successive onsets and auroral re-intensifications, the active expansion phase aurora persisted for more than 1 hr and spanned a region of over 6 MLT, with a poleward extent of approximately ∼5°.

4. Discussion and Summary

Numerous studies have investigated the onset process of substorms, but limited studies have focused on the spatiotemporal development of the substorm expansion phase (e.g., Lyons & Nishimura, 2020 and reference therein). Given that the expansion phase is highly variable in both spatial and temporal domains and is a period of large-scale energy dissipation in the ionosphere, it is crucial to study the spatiotemporal development of expansion phase aurora in detail. Taking advantage of the continent-scale THEMIS ASIs and extensive coverage of magnetometers, we investigated the spatiotemporal evolution of substorm expansion phase aurora during both single-onset and multiple-onset auroral substorms. By analyzing seven events, we aimed to investigate the auroral enhancements contributing to the prolonged expansion phase, determining whether these enhancements are new auroral onsets, prolonged PBIs, or expansion-phase auroral streamers.

In multiple-onset auroral substorms, the initial auroral substorm onset is followed by successive auroral onsets. The active aurora from the successive onset merges with the active aurora from the previous onset, enhancing the spatial extent and duration of the aurora. The successive onsets may appear similar to the initial onset and can occur anywhere between 5 and 30 min after the previous auroral onset. They can occur eastward, westward, and poleward of the initial onset, resulting in step-wise azimuthal and poleward expansion of the onset aurora. The successive onsets were accompanied by the Pi2 pulsations and may be associated with a step-like decrease in the SML index during the expansion phase, resulting in the prolonged occurrence of negative bay in the SML index. Based on the analysis of seven events, we could not ascertain a distinct preference for specific IMF conditions that distinguish single-onset from multiple-onset substorms. A more comprehensive study involving a larger data set or different IMF parameters might provide further insight into any IMF preference for single and multiple-onset substorms.

If successive onsets are the only process determining the spatiotemporal development of the substorm expansion phase, then single-onset substorms may be expected to be of smaller scale (in both spatial and temporal domains) compared to multiple-onset substorms. For instance, the expansion phase of Event#1 and 2, which were not accompanied by prolonged PBIs and streamers, were of short duration (last for ∼5–10 min), longitudinally localized (remain confined around the onset longitude) and showed smaller drop in the SML index. However, the spatiotemporal development of single-onset substorms (Event 3# 16 February 2010) can resemble the multiple-onset substorms. Such single-onset auroral substorm may exhibit a large expansion phase that consists of prolonged expansion phase auroral streamers, creating a large drop in the magnetic field. In addition, for the single-onset substorm of Event#3, the auroral observations revealed a 50 min long sequence of PBIs comprising two distinct PBI events, feeding the substorm expansion phase. The multiple-onset substorms also consisted of multiple episodes of prolonged PBIs, suggesting the crucial role of prolonged PBIs and streamers in shaping the substorm expansion phase. The selected examples presented in this study illustrate the role of prolonged PBIs and ensuing streamers, alongside successive onsets, and the frequent occurrence of various combinations of these features.

Observations reveal some PBIs exhibit an abrupt poleward expansion (poleward explosion) and contributed to the formation of a westward-expanding surge, resulting in the development of a longitudinally extended PBI covering

approximately a 3 MLT wide region. For instance, in the case of multiple-onset substorm event on 11 March 2008, a sudden brightening and explosion of PBI triggered an abrupt poleward expansion, followed by the formation of a longitudinally extended (∼3 MLT wide) PBI. The poleward explosions of PBIs were associated with a drop in the magnetic field, SML index, and Pi2 pulsations, similar to the characteristics observed during substorm auroral onsets. It's worth reiterating that relying solely on magnetometer data, the event of poleward explosion and prolonged sequence of PBIs might be mistaken for a new successive onset. These results further suggest that the large-scale magnetospheric energy release during substorms can occur in two ways: (a) by causing multiple onsets and (b) by inducing PBIs and ensuing auroral streamers. It could be a subject for future investigation to determine (a) why certain substorms exhibit a large expansion phase with a broader MLT extent, while others begin with a smaller expansion phase and evolve into a broader MLT extent through successive onsets or prolonged PBIs, leading to step-wise poleward/azimuthal expansion, (b) what are the conditions under which prolonged PBIs accompany substorm expansion phase.

Previous studies have shown that PBIs are associated with equatorward-directed flow channels traversing the poleward boundary of the auroral oval from the polar cap (de la Beaujardière et al., 1994; Shi et al., 2012; Zou et al., 2014). Ohtani et al. (2018) demonstrated the formation of longitudinally extended PBIs and proposed that longitudinal ionospheric convection is crucial in their formation and development. Lyons et al. (2011) used radar observations to reveal meso-scale flows within the polar cap, moving toward the nightside boundary before substorm onset. They suggested that these flows contribute to triggering PBIs and streamers. Flow channels from the polar cap can reach the nightside open-closed boundary, potentially triggering plasma sheet flow bursts, and may play a key role in both pre- and post-onset auroral activity (Nishimura et al., 2013). These studies proposed the possibility that such flow channels occurring after substorm onset play a significant role in the post-onset auroral poleward expansion and the duration of post-onset auroral activity—a proposal that has remained un-explored so far. The auroral observations presented in our study evidently show that the post-onset PBIs and streamers play a crucial role in driving the spatiotemporal development of the substorm expansion phase. Therefore, our findings contribute to advancing our understanding of the factors influencing the spatiotemporal evolution of the substorm expansion phase, taking a significant step toward addressing this longstanding question. Future studies should use radar data to confirm the role of flow channels originating from the polar cap in the formation of longitudinally extended PBIs, which contribute to sustaining the expansion phase aurora.

Another interesting aspect this study highlights is the re-intensification of active auroral bulge (Event#7) immediately equatorward of the PBA. Lyons, Liu, Nishimura, Wang, et al. (2021) demonstrated the presence of flow channels adjacent to the PBA. Ma et al. (2021) suggested that flow channels originating from the polar cap feed the surge formation and drive the WTS. They showed that auroral streamers with an adjacent flow channel that feed the low-entropy plasma into surge development are connected to the auroral polar boundary. That the localized polar cap flow adjacent to the polar boundary arc set off the WTS was also illustrated by Lyons, Nishimura, Gallardo-Lacourt, et al. (2013) and Lyons, Liu, Nishimura, Wang, et al. (2021). However, what we observed in the present study is that the re-intensification of active substorm auroral bulge occurred immediately equatorward of the PBA. These findings suggest that flow channels associated with PBAs may supply new plasma to the auroral surge, leading to further intensifications. In addition, we observed the onset of substorm when the equatorward moving PBA approached the growth-phase arc (Event#1 and 7). While our observations offer new insight into the role of auroral poleward boundary in driving spatiotemporal development of substorm expansion phase, further investigation on this aspect is warranted. A dedicated study focusing on this aspect is currently underway.

In this study, we also examined whether the successive onsets were preceded by the post-onset streamers, like the substorm onset, which is generally preceded by pre-onset streamers (Lyons et al., 2010; Nishimura, Lyons, Zou, Angelopoulos, & Mende, 2010; Nishimura, Lyons, Zou, Xing, et al., 2010). Previous studies showed that the equatorward flow channels lie east of the streamer (Gallardo-Lacourt et al., 2014; Lyons, Gallardo-Lacourt, & Nishimura, 2022; Lyons, Nishimura, et al., 2022; Sergeev et al., 2004). The auroral observations presented in this study show that the post-onset streamers during the substorm expansion phase may trigger multiple onsets at different longitudes. As discussed above, these onsets lead to substantial azimuthal broadening of expansion activity as well as prolonging the expansion phase duration. This is likely an important cause of the large variety of expansion phase coverage areas and durations. However, not all post-onset streamers trigger successive onsets, as clearly observed in the present study, such as event #6. Previous research (e.g., Nishimura et al., 2011) has shown that pre-onset streamers do not always lead to substorm onset. Therefore, it is important to investigate the

underlying conditions under which post-onset streamers result in successive onsets. Further, in some cases, it is not clear if the streamer contacted the growth phase arc, the onset occurring somewhat equatorward of the streamer. Consistent with this, the onset of substorms may occur when the pre-onset streamer does not reach all the way to the growth-phase arc (e.g., Nishimura et al., 2011). This is as expected, because an optical contact between the streamer and growth phase arc is not necessary. A streamer demarcates an adjacent flow channel, and the plasma within the flow channel is expected to directly connect to the onset location along the growth phase arc (Lyons & Nishimura, 2020).

Data Availability Statement

- THEMIS data can be obtained online at https://cdaweb.gsfc.nasa.gov/pub/data/themis/.
- SuperMAG ground magnetometer and SML data can be obtained at supermag.jhuapl.edu.
- Solar wind parameters (IMF Bz) were obtained from the SPDF, NASA, USA at http://omniweb.gsfc.nasa.gov.
- Space Physics Environment Data Analysis Software (SPEDAS) tool, which is used to download and analyze the data, can be downloaded from https://spedas.org/blog/.

Acknowledgments

We acknowledge use of the SuperMAG ground magnetometer station data (Gjerloev, 2012) and SuperMAG SML and SMU data (Newell & Gjerloev, 2011). We also acknowledge all SuperMAG collaborators (https://supermag.jhuapl.edu/info/?page=acknowledgement). We acknowledge (a) NASA Contract NAS5-02099 and V. Angelopoulos for use of data from the THEMIS Mission. (b) S. Mende and E. Donovan for use of the ASI data, the CSA for logistical support in fielding and data retrieval from the GBO stations, and NSF for support of GIMNAST through Grant AGS-1004736. (c) S. Mende and C. T. Russell for use of the UCLA GMAG data (Russell et al., 2008) and NSF for support through Grant AGS-1004814. (d) I. R. Mann, D. K. Milling and the rest of the CARISMA team for use of CARISMA GMAG data (Mann et al., 2008). CARISMA is operated by the University of Alberta, funded by the Canadian Space Agency. (e) Martin Connors and C. T. Russell and the rest of the AUTUMN/AUTUMNX team for use of the GMAG data. (f) US Geological Survey magnetometers (USGS), original data provided by the USGS Geomagnetism Program (http://geomag.usgs.gov). (g) The Canadian Magnetic Observatory Network (CANMON), maintained and operated by the Geological Survey of Canada, provided the data used in this study (http://www.geomag.nrcan.gc.ca). (h) Peter Chi for use of the McMAC data and NSF for support through Grant ATM-0245139. Work at UCLA has been supported by NSF Grant 2055192, NASA Grants 80NSSC20K1314, 80NSSC20K1316, and 80NSSC22K0751. Work at Boston University was supported by NASA Grants 80NSSC18K0657, 80NSSC20K0604, 80NSSC20K0725, 80NSSC21K1321, 80NSSC22K0323, 80NSSC22K0749, and 80NSSC19K0546, NSF Grants AGS-1907698 and AGS-2100975, and AFOSR Grant FA9559-16-1-0364. Work at APL was supported by NSF AGS-195292, NSF AGS-2120503, and the NASA DRIVE Science Center for Geospace Storms (CGS) under Award 80NSSC22M0163.

References

Aikio, A. T., Pitkanen, T., Kozlovsky, A., & Amm, O. (2006). Method to locate the polar cap boundary in the nightside ionosphere and application to a substorm event. *Annales Geophysicae*, *24*(7), 1905–1917. https://doi.org/10.5194/angeo-24-1905-2006

Aikio, A. T., Sergeev, V. A., Shukhtina, M. A., Vagina, L. I., Angelopoulos, V., & Reeves, G. D. (1999). Characteristics of pseudobreakups and substorms observed in the ionosphere, at the geosynchronous orbit, and in the midtail. *Journal of Geophysical Research*, *104*(A6), 12263–12287. https://doi.org/10.1029/1999JA900118

Akasofu, S.-I., Kimball, D. S., & Meng, C.-I. (1965). The dynamics of the aurora. II. Westward traveling surges. *Journal of Atmospheric and Terrestrial Physics*, *27*(2), 173–187. https://doi.org/10.1016/0021-9169(65)90114-5

Angelopoulos, V. (2008). The THEMIS mission. *Space Science Reviews*, *141*(1–4), 5–34. https://doi.org/10.1007/s11214-008-9336-1

Angelopoulos, V., Cruce, P., Drozdov, A., Grimes, E. W., Hatzigeorgiu, N., King, D. A., et al. (2019). The space physics environment data analysis system (SPEDAS). *Space Science Reviews*, *215*(1), 9. https://doi.org/10.1007/s11214-018-0576-4

Chu, X., McPherron, R. L., Hsu, T.-S., & Angelopoulos, V. (2015). Solar cycle dependence of substorm occurrence and duration: Implications for onset. *Journal of Geophysical Research: Space Physics*, *120*(4), 2808–2818. https://doi.org/10.1002/2015JA021104

de la Beaujardière, O., Lyons, L. R., Ruohoniemi, J. M., Friis-Christensen, E., Danielsen, C., Rich, F. J., & Newell, P. T. (1994). Quiet-time intensifications along the poleward auroral boundary near midnight. *Journal of Geophysical Research*, *99*(A1), 287–298. https://doi.org/10.1029/93JA01947

Despirak, I. V., Lubchich, A. A., & Guineva, V. (2011). Development of substorm bulges during storms of different interplanetary origins. *Journal of Atmospheric and Solar-Terrestrial Physics*, *73*(11–12), 1460–1464. https://doi.org/10.1016/j.jastp.2010.08.003

Donovan, E., Mende, S., Jackel, B., Frey, H., Syrjäsuo, M., Voronkov, I., et al. (2006). The THEMIS all-sky imaging array—System design and initial results from the prototype imager. *Journal of Atmospheric and Solar-Terrestrial Physics*, *68*(13), 1472–1487. https://doi.org/10.1016/j.jastp.2005.03.027

Elphinstone, R. D., Murphree, J. S., & Cogger, L. L. (1996). What is a global auroral substorm? *Reviews of Geophysics*, *34*(2), 169–232. https://doi.org/10.1029/96rg00483

Forsyth, C., Rae, I. J., Coxon, J. C., Freeman, M. P., Jackman, C. M., Gjerloev, J., & Fazakerley, A. (2015). A new technique for determining substorm onsets and phases from indices of the electrojet (SOPHIE). *Journal of Geophysical Research: Space Physics*, *120*(12), 10592–10606. https://doi.org/10.1002/2015JA021343

Gallardo-Lacourt, B., Nishimura, Y., Lyons, L. R., Zou, S., Angelopoulos, V., Donovan, E., et al. (2014). Coordinated SuperDARN THEMIS ASI observations of mesoscale flowbursts associated with auroral streamers. *Journal of Geophysical Research: Space Physics*, *119*(1), 142–150. https://doi.org/10.1002/2013JA019245

Gjerloev, J. W. (2012). The SuperMAG data processing technique. *Journal of Geophysical Research*, *117*(A9), A09213. https://doi.org/10.1029/2012JA017683

Gjerloev, J. W., Hoffman, R. A., Sigwarth, J. B., & Frank, L. A. (2007). Statistical description of the bulge-type auroral substorm in the far ultraviolet. *Journal of Geophysical Research*, *112*(A7), A07213. https://doi.org/10.1029/2006JA012189

Henderson, M. G. (2012). Auroral substorms, poleward boundary activations, auroral streamers, omega bands, and onset precursor activity. In A. Keiling, E. Donovan, F. Bagenal, & T. Karlsson (Eds.), *Auroral phenomenology and magnetospheric processes: Earth and other planets, Geophysical Monograph Series* (Vol. 197, pp. 39–54). American Geophysical Union. https://doi.org/10.1029/2011GM001165

Henderson, M. G., Reeves, G. D., & Murphree, J. S. (1994). The activation of the dusk-side and the formation of north-south aligned structures during substorms In J. R. Kan, J. D. Craven, & S.-I. Akasofu (Eds.), *Proc. Second international conference on substorms (ICS-2)* (p. 37). Geophysical Institute, University of Alaska Fairbanks.

Henderson, M. G., Reeves, G. D., & Murphree, J. S. (1998). Are north-south aligned auroral structures an ionospheric manifestation of bursty bulk flows? *Geophysical Research Letters*, *25*(19), 3737–3740. https://doi.org/10.1029/98gl02692

Ieda, A., Nishimura, Y., Miyashita, Y., Angelopoulos, V., Runov, A., Nagai, T., et al. (2016). Stepwise tailward retreat of magnetic reconnection: THEMIS observations of an auroral substorm. *Journal of Geophysical Research: Space Physics*, *121*(5), 4548–4568. https://doi.org/10.1002/2015JA022244

Jacobs, J. A., Kato, Y., Matsushita, S., & Troitskaya, V. A. (1964). Classification of geomagnetic micropulsations. *Journal of Geophysical Research*, *69*(1), 180–181. https://doi.org/10.1029/JZ069i001p00180

Kauristie, K., Sergeev, V. A., Kubyshkina, M., Pulkkinen, T. I., Angelopoulos, V., Phan, T., et al. (2000). Ionospheric current signatures of transient plasma sheet flows. *Journal of Geophysical Research*, *105*(A5), 10677–10690. https://doi.org/10.1029/1999JA900487

Keiling, A., & Takahashi, K. (2011). Review of Pi2 models. *Space Science Reviews*, *161*(1–4), 63–148. https://doi.org/10.1007/s11214-011-9818-4

Kepko, L., Spanswick, E., Angelopoulos, V., Donovan, E., McFadden, J., Glassmeier, K.-H., et al. (2009). Equatorward moving auroral signatures of a flow burst observed prior to auroral onset. *Geophysical Research Letters*, *36*(24), L24104. https://doi.org/10.1029/2009GL041476

Kim, K.-H., Takahashi, K., Lee, D.-H., Sutcliffe, P. R., & Yumoto, K. (2005). Pi2 pulsations associated with poleward boundary intensifications during the absence of substorms. *Journal of Geophysical Research*, *110*(A1), A01217. https://doi.org/10.1029/2004JA010780

Kisabeth, J. L., & Rostoker, G. (1971). Development of polar electrojet during polar magnetic substorms. *Journal of Geophysical Research*, *76*(28), 6815–6828. https://doi.org/10.1029/JA076i028p06815

Kisabeth, J. L., & Rostoker, G. (1974). Expansive phase of magnetospheric substorms: 1. Development of auroral electrojets and auroral arc configuration during a substorm. *Journal of Geophysical Research*, *79*(7), 972–984. https://doi.org/10.1029/JA079i007p00972

Lyons, L. R., Gallardo-Lacourt, B., & Nishimura, Y. (2022). Auroral structures: Revealing the importance of meso-scale M-I coupling. In Y. Nishimura, O. Verkhoglyadova, Y. Deng, & S. R. Zhang (Eds.), *Cross-scale coupling and energy transfer in the magnetosphere-ionosphere-thermosphere system* (pp. 65–101). Elsevier. https://doi.org/10.1016/B978-0-12-821366-7.00004-4

Lyons, L. R., Liu, J., Nishimura, Y., Reimer, A. S., Bristow, W. A., Hampton, D. L., et al. (2021). Radar observations of flows leading to substorm onset over Alaska. *Journal of Geophysical Research: Space Physics*, *126*(2), e2020JA028147. https://doi.org/10.1029/2020JA028147

Lyons, L. R., Liu, J., Nishimura, Y., Wang, C.-P., Reimer, A. S., Bristow, W. A., et al. (2021). Radar observations of flows leading to longitudinal expansion of substorm onset over Alaska. *Journal of Geophysical Research: Space Physics*, *126*(2), e2020JA028148. https://doi.org/10.1029/2020JA028148

Lyons, L. R., Nagai, T., Blanchard, G. T., Samson, J. C., Yamamoto, T., Mukai, T., et al. (1999). Association between Geotail plasma flows and auroral poleward boundary intensifications observed by CANOPUS photometers. *Journal of Geophysical Research*, *104*(A3), 4485–4500. https://doi.org/10.1029/1998JA900140

Lyons, L. R., & Nishimura, Y. (2020). Substorm onset and development: The crucial role of flow channels. *Journal of Atmospheric and Solar-Terrestrial Physics*, *211*, 105474. https://doi.org/10.1016/j.jastp.2020.105474

Lyons, L. R., Nishimura, Y., Donovan, E., & Angelopoulos, V. (2013). Distinction between auroral substorm onset and traditional ground magnetic onset signatures. *Journal of Geophysical Research: Space Physics*, *118*(7), 4080–4092. https://doi.org/10.1002/jgra.50384

Lyons, L. R., Nishimura, Y., Gallardo-Lacourt, B., Zou, Y., Donovan, E., Mende, S., et al. (2013). Westward traveling surges: Sliding along boundary arcs and distinction from onset arc brightening. *Journal of Geophysical Research: Space Physics*, *118*(12), 7643–7653. https://doi.org/10.1002/2013JA019334

Lyons, L. R., Nishimura, Y., Kim, H.-J., Donovan, E., Angelopoulos, V., Sofko, G., et al. (2011). Possible connection of polar cap flows to pre- and post-substorm onset PBIs and streamers. *Journal of Geophysical Research*, *116*(A12), 14. https://doi.org/10.1029/2011JA016850

Lyons, L. R., Nishimura, Y., Liu, J., Bristow, W. A., Zou, Y., & Donovan, E. F. (2022). Verification of substorm onset from intruding flow channels with high-resolution SuperDARN radar flow maps. *Journal of Geophysical Research: Space Physics*, *127*(8), e2022JA030723. https://doi.org/10.1029/2022JA030723

Lyons, L. R., Nishimura, Y., Shi, Y., Zou, S., Kim, H.-J., Angelopoulos, V., et al. (2010). Substorm triggering by new plasma intrusion: Incoherent-scatter radar observations. *Journal of Geophysical Research*, *115*(A7), A07223. https://doi.org/10.1029/2009JA015168

Ma, Y.-Z., Zhang, Q.-H., Lyons, L. R., Liu, J., Xing, Z.-Y., Reimer, A., et al. (2021). Is westward travelling surge driven by the polar cap flow channels? *Journal of Geophysical Research: Space Physics*, *126*(8), e2020JA028498. https://doi.org/10.1029/2020JA028498

Mann, I. R., Milling, D. K., Rae, I. J., Ozeke, L. G., Kale, A., Kale, Z. C., et al. (2008). The upgraded CARISMA magnetometer array in the THEMIS era. *Space Science Reviews*, *141*(1–4), 413–451. https://doi.org/10.1007/s11214-008-9457-6

McPherron, R. L. (1979). Magnetospheric substorms. *Reviews of Geophysics*, *17*(4), 657–681. https://doi.org/10.1029/RG017i004p00657

Mende, S. B., Harris, S. E., Frey, H. U., Angelopoulos, V., Russell, C. T., Donovan, E., et al. (2008). The THEMIS array of ground-based observatories for the study of auroral substorms. *Space Science Reviews*, *141*(1–4), 357–387. https://doi.org/10.1007/s11212-008-9380-x

Montbriand, L. E. (1971). The proton aurora substorm. In B. M. McCormac (Ed.), *The radiating atmosphere* (pp. 366–373). D. Reidel.

Nakamura, R., Baumjohann, W., Schödel, R., Brittnacher, M., Sergeev, V. A., Kubyshkina, M., et al. (2001). Earthward flow bursts, auroral streamers, and small expansions. *Journal of Geophysical Research*, *106*(A6), 10791–10802. https://doi.org/10.1029/2000JA000306

Nakamura, R., Oguti, T., Yamamoto, T., & Kokubun, S. (1993). Equatorward and poleward expansion of the auroras during auroral substorms. *Journal of Geophysical Research*, *98*(A4), 5743–5759. https://doi.org/10.1029/92JA02230

Newell, P. T., & Gjerloev, J. W. (2011). Evaluation of SuperMAG auroral electrojet indices as indicators of substorms and auroral power. *Journal of Geophysical Research*, *116*(A12), A12211. https://doi.org/10.1029/2011JA016779

Nishimura, Y., Lyons, L., Gabrielse, C., Sivadas, N., Donovan, E., Varney, R., et al. (2020). Extreme magnetosphere-ionosphere-thermosphere responses to the 5 April 2010 supersubstorm. *Journal of Geophysical Research: Space Physics*, *125*(4), e2019JA027654. https://doi.org/10.1029/2019ja027654

Nishimura, Y., Lyons, L., Zou, S., Angelopoulos, V., & Mende, S. (2010). Substorm triggering by new plasma intrusion: THEMIS all-sky imager observations. *Journal of Geophysical Research*, *115*(A7), A07222. https://doi.org/10.1029/2009ja015166

Nishimura, Y., Lyons, L. R., Kikuchi, T., Angelopoulos, V., Donovan, E., Mende, S., et al. (2012). Formation of substorm Pi2: A coherent response to auroral streamers and currents. *Journal of Geophysical Research*, *117*(A9), A09218. https://doi.org/10.1029/2012ja017889

Nishimura, Y., Lyons, L. R., Shiokawa, K., Angelopoulos, V., Donovan, E. F., & Mende, S. B. (2013). Substorm onset and expansion phase intensification precursors seen in polar cap patches and arcs. *Journal of Geophysical Research: Space Physics*, *118*(5), 2034–2042. https://doi.org/10.1002/jgra.50279

Nishimura, Y., Lyons, L. R., Zou, S., Angelopoulos, V., & Mende, S. B. (2011). *Categorization of the time sequence of events leading to substorm onset based on THEMIS all-sky imager observations* (pp. 133–142). Springer-Verlag Berlin. https://doi.org/10.1007/978-94-007-0501-2_8

Nishimura, Y., Lyons, L. R., Zou, S., Xing, X., Angelopoulos, V., Mende, S. B., et al. (2010). Preonset time sequence of auroral substorms: Coordinated observations by all-sky imagers, satellites, and radars. *Journal of Geophysical Research*, *115*(A5), A00I08. https://doi.org/10.1029/2010JA015832

Ohtani, S., Gjerloev, J. W., McWilliams, K. A., Ruohoniemi, J. M., & Frey, H. U. (2021). Simultaneous development of multiple auroral substorms: Double auroral bulge formation. *Journal of Geophysical Research: Space Physics*, *126*(5), e2020JA028883. https://doi.org/10.1029/2020JA028883

Ohtani, S., Motoba, T., Gjerloev, J. W., Frey, H. U., Mann, I. R., Chi, P. J., & Korth, H. (2022). New insights into the substorm initiation sequence from the spatio-temporal development of auroral electrojets. *Journal of Geophysical Research: Space Physics*, *127*(6), e2021JA030114. https://doi.org/10.1029/2021JA030114

Ohtani, S., Motoba, T., Gjerloev, J. W., Ruohoniemi, J. M., Donovan, E. F., & Yoshikawa, A. (2018). Longitudinal development of poleward boundary intensifications (PBIs) of auroral emission. *Journal of Geophysical Research: Space Physics*, *123*(11), 9005–9021. https://doi.org/10.1029/2017JA024375

Olson, J. V. (1999). Pi2 pulsations and substorm onsets: A review. *Journal of Geophysical Research*, *104*(A8), 17499–17520. https://doi.org/10.1029/1999ja900086

Perraut, S., Le Contel, O., Roux, A., Parks, G., Chua, D., Hoshino, M., & Nagai, T. (2003). Substorm expansion phase: Observations from Geotail, Polar and IMAGE network. *Journal of Geophysical Research*, *108*(A4), 1159. https://doi.org/10.1029/2002ja009376

Pytte, T., McPherron, R. L., & Kokubun, S. (1976). The ground signatures of the expansion phase during multiple onset substorms. *Planetary and Space Science*, *24*(12), 1115–1132. https://doi.org/10.1016/0032-0633(76)90149-5

Rostoker, G., Akasofu, S. I., Foster, J., Greenwald, R., Kamide, Y., Kawasaki, K., et al. (1980). Magnetospheric substorm-definition and signatures. *Journal of Geophysical Research*, *85*(A4), 1663–1668. https://doi.org/10.1029/ja085ia04p01663

Russell, C. T., Chi, P. J., Dearborn, D. J., Ge, Y. S., Kuo-Tiong, B., Means, J. D., et al. (2008). THEMIS ground-based magnetometers. *Space Science Reviews*, *141*(1–4), 389–412. https://doi.org/10.1007/s11214-008-9337-0

Saito, T., Yumoto, K., & Koyama, Y. (1976). Magnetic pulsation Pi2 as a sensitive indicator of magnetospheric substorm. *Planetary and Space Science*, *24*(11), 1025–1029. https://doi.org/10.1016/0032-0633(76)90120-3

Sergeev, V. A., Liou, K., Meng, C.-I., Newell, P. T., Brittnacher, M., Parks, G., & Reeves, G. D. (1999). Development of auroral streamers in association with localized impulsive injections to the inner magnetotail. *Geophysical Research Letters*, *26*(3), 417–420. https://doi.org/10.1029/1998GL900311

Sergeev, V. A., Liou, K., Newell, P. T., Ohtani, S. I., Hairston, M. R., & Rich, F. (2004). Auroral streamers: Characteristics of associated precipitation, convection and field-aligned currents. *Annales Geophysicae*, *22*(2), 537–548. https://doi.org/10.5194/angeo-22-537-2004

Sergeev, V. A., Sauvaud, J.-A., Popescu, D., Kovrazhkin, R. A., Liou, K., Newell, P. T., et al. (2000). Multiple-spacecraft observation of a narrow transient plasma jet in the Earth's plasma sheet. *Geophysical Research Letters*, *27*(6), 851–854. https://doi.org/10.1029/1999GL010729

Sergeev, V. A., & Yahnin, A. G. (1979). Features of auroral bulge expansion. *Planetary and Space Science*, *27*(12), 1429–1440. https://doi.org/10.1016/0032-0633(79)90089-8

Shi, Y., Zesta, E., Lyons, L. R., Xing, X., Angelopoulos, V., Donovan, E., et al. (2012). Multipoint observations of substorm pre-onset flows and time sequence in the ionosphere and magnetosphere. *Journal of Geophysical Research*, *117*(A9), A09203. https://doi.org/10.1029/2011JA017185

Sutcliffe, P., & Lyons, L. (2002). Association between quiet-time Pi2 pulsations, poleward boundary intensifications, and plasma sheet particle fluxes. *Geophysical Research Letters*, *29*(9), 1293. https://doi.org/10.1029/2001GL014430

Wiens, R. G., & Rostoker, G. (1975). Characteristics of development of westward electrojet during expansive phase of magnetospheric substorms. *Journal of Geophysical Research*, *80*(16), 2109–2128. https://doi.org/10.1029/JA080i016p02109

Yadav, S., Lyons, L. R., Liu, J., Nishimura, Y., Tian, S., Zou, Y., & Donovan, E. F. (2022). Association of equatorward extending auroral streamers with ground magnetic perturbations and geosynchronous injections. *Journal of Geophysical Research: Space Physics*, *127*(11), e2022JA030919. https://doi.org/10.1029/2022JA030919

Zesta, E., Lyons, L., & Donovan, E. (2000). The auroral signature of earthward flow bursts observed in the magnetotail. *Geophysical Research Letters*, *27*(20), 3241–3244. https://doi.org/10.1029/2000gl000027

Zou, Y., Nishimura, Y., Lyons, L. R., Donovan, E. F., Ruohoniemi, J. M., Nishitani, N., & McWilliams, K. A. (2014). Statistical relationships between enhanced polar cap flows and PBIs. *Journal of Geophysical Research: Space Physics*, *119*(1), 151–162. https://doi.org/10.1002/2013JA019269